University of Nevada, Reno

The Development of Diagnostic Immunoassays for Melioidosis and Ebola Virus Disease

A dissertation submitted in partial fulfillment of the requirements for the degree of Doctor of Philosophy in Cellular and Molecular Biology

By

Heather R. Green

Dr. David P. AuCoin | Dissertation Advisor

May 2022

THE GRADUATE SCHOOL

We recommend that the dissertation
prepared under our supervision by

HEATHER R. GREEN

entitled

The Development of Diagnostic Immunoassays for Melioidosis and Ebola Virus Disease

be accepted in partial fulfillment of the
requirements for the degree of

DOCTOR OF PHILOSOPHY

David P. AuCoin, Ph.D.
Advisor

Mary N. Burtnick, Ph.D.
Committee Member

Cyprian C. Rossetto, Ph.D.
Committee Member

Subhash C. Verma, Ph.D.
Committee Member

Dean J. Burkin, Ph.D.
Graduate School Representative

David W. Zeh, Ph.D., Dean
Graduate School

May, 2022

Abstract

Burkholderia pseudomallei and five species of Ebola virus (EBOV) are the causative agents of melioidosis and Ebola virus disease (EVD), respectively. Melioidosis and EVD are deadly infectious diseases with high mortality rates. Furthermore, both pathogens are regulated under the United States of America Federal Select Agent Program due to their potential to be used in bioterrorism. Early diagnosis is imperative for treating the specific disease as well as minimizing the spread of the pathogen. Diagnostic measures for both diseases rely on identification of the causative agent or identifying a humoral response against the causative agent. For melioidosis, the current gold standard for diagnosing an infection is through isolating the bacteria by culturing. For EVD, the current diagnostic measures include polymerase chain reaction (PCR) to identify viral nucleic acid and enzyme-linked immunosorbent assay (ELISA) for the detection of viral antigens or antibodies reactive to EBOV antigens. All three diagnostic assays can take several hours to days to get a result, require specialized training, and access to expensive equipment. The areas in which both pathogens cause the highest global burden are typically resource poor areas including Southeast Asia and northern Australia for *B. pseudomallei* and West Africa for Ebola virus. More rapid diagnostic methods would greatly improve the morbidity and mortality associated with these diseases. Lateral flow immunoassays (LFIs) are rapid, point-of-care (POC) diagnostic tools that utilize antibodies and colorimetry to detect a biomarker for a specific disease or other condition. This dissertation outlines alternative approaches to enhance the detection of *B. pseudomallei* capsular polysaccharide (CPS) on an LFI as well as outlines the development of a prototype LFI for the rapid diagnosis of early EVD through detection of Ebola virus soluble glycoprotein (sGP).

The Active Melioidosis *Detect*™ Lateral Flow Immunoassay (AMD LFI) was developed by our laboratory in collaboration with InBios International, Inc. (Seattle, WA) to diagnose melioidosis through the detection of CPS, a biomarker of the disease. The AMD LFI has high specificity and analytical sensitivity, but the clinical sensitivity can be low depending on the sample type. testing of some patient samples on this assay indicated that it was not sensitive enough to detect all clinically relevant concentrations of CPS. Here we developed a magnetic immunoprecipitation method for the pre-concentration of CPS from melioidosis patient urine samples to enrich these samples for CPS. CPS reactive monoclonal antibody (mAb) 4C4 was conjugated to magnetic particles and a protocol was developed utilizing acid-base elution neutralization chemistry. We have shown that this protocol resulted in increased AMD LFI positivity when testing melioidosis patient urine samples.

Passive concentration of *Burkholderia pseudomallei* CPS was also explored as an alternative method to enrich the sample for CPS prior to evaluating on the AMD LFI for a less labor-intensive approach. Following a melioidosis diagnosis, patients were actively enrolled into a study in which they provided urine and/or serum samples to be tested on the AMD LFI. These samples underwent extensive testing, including culturing to identify if *B. pseudomallei* was present at the time of sample collection as well LFI testing. Urine samples were tested on the AMD LFI, as well as serum samples from some patients for a direct comparison. Urine was found to be the optimal matrix for CPS detection in confirmed melioidosis patient samples as in general it appeared urine contained higher concentrations of CPS when compared to blood samples from the same patient taken at nearly the same time. Furthermore, we found that passive concentration of urine resulted

in stronger test line intensity on the AMD LFI as well as provided more positive results than when testing serum or unconcentrated urine.

Lastly, antibody-based immunoassays were developed for detection of EBOV sGP, a well-established biomarker of an Ebola virus infection. Current diagnostic assays for EVD focus on detection of glycoprotein (GP) and viral matrix protein (VP40), but sGP may have the potential to be a superior biomarker. sGP and GP are encoded by the same gene, *GP*, and sGP is the main product of *GP.* Furthermore, large amounts of sGP can be detected in the bloodstream early during an Ebola virus disease infection. Splenocytes were isolated from mice immunized with either sGP or Ebola virus-like particles (VLPs), and hybridoma technology was utilized to establish immortalized cell lines that produced sGP reactive antibodies. This work resulted in the isolation of a library of seventeen high affinity mAbs that are reactive to EBOV sGP. These mAbs were characterized via Western immunoblotting, direct and antigen-capture ELISA, surface plasmon resonance, and lateral flow immunoassay. Prototype antigen-capture ELISA and LFIs were developed and optimized using pairs of mAbs isolated in this study.

Acknowledgments

I would like to thank my advisor, Dr. David AuCoin. I am grateful for the opportunity to pursue my PhD in his laboratory and appreciate all the support and mentorship I received over the years. I would also like to thank my committee members Dr. Mary Burtnick, Dr. Cyprian Rossetto, Dr. Subhash Verma, and Dr. Dean Burkin for imparting their knowledge, as well as supporting and guiding me through this process.

I would like to thank all past and present members of the Diagnostics Discovery Laboratory. I am thankful for everyone who contributed to my growth as a scientist and for their continued support.

I would like to thank my family for always believing in me and encouraging me. An extra special thanks to my partner, Michael, who was everything I needed him to be and more throughout this process. And finally, to Floki, the sassy husky who couldn't be bothered to greet me like a normal dog on those extra rough days, you suck, but I love you anyways.

Table of Contents

PAGE

Abstract i

Acknowledgements iv

Table of Contents v

List of Tables viii

List of Figures ix

Chapter 1: Introduction 1

1.1 Overview

1.2 *Burkholderia pseudomallei* and Melioidosis

1.3 Ebola virus and Ebola Virus Disease

1.4 Antibodies

1.5 Diagnostic Immunoassays

1.6 Figures

Chapter 2: Magnetic immunoprecipitation for concentrating *Burkholderia pseudomallei* capsular polysaccharide 22

2.1 Abstract

2.2 Background

2.3 Methods

2.4 Results

2.5 Discussion

2.6 Figures and Tables

Chapter 3: Passive concentration of *Burkholderia pseudomallei* capsular polysaccharide from melioidosis urine samples for the enhanced detection on the Active Melioidosis Detect Lateral Flow Immunoassay.....49

3.1 Abstract

3.2 Background

3.3 Methods

3.4 Results

3.5 Discussion

3.6 Figures and Tables

Chapter 4: Development of a lateral flow immunoassay for the detection of Ebola virus soluble glycoprotein.....82

4.1 Abstract

4.2 Background

4.3 Methods

4.4 Results

4.5 Discussion

4.6 Figures and Tables

Chapter 5: Conclusion.....109

Literature Cited 115

List of Tables

Chapter 2: Magnetic immunoprecipitation for concentrating *Burkholderia pseudomallei* capsular polysaccharide

Table 1	CPS quantification and AMD Plus LFI results of 1 mL human melioidosis samples obtained from Menzies School of Health Research	45
Table 2	CPS quantification and AMD Plus LFI results of 10 mL human melioidosis samples obtained from Lao-Oxford-Mahost Hospital-Wellcome Trust Research	46

Chapter 3: Passive concentration of *Burkholderia pseudomallei* capsular polysaccharide from melioidosis urine samples for the enhanced detection on the Active Melioidosis *Detect*™ lateral flow immunoassay

Table 1	Summary of the *E. coli* and *K. pneumoniae* confirmed patient samples and results of urine samples tested on the AMD Plus LFI at the Naval Health Research Center, before and after concentrating	73
Table 2	Summary of the patient samples and results of urine samples tested on the AMD Plus LFI at the Menzies Health Center, before and after concentrating	75
Table 3	Summary of the patient samples and results of urine samples tested on the AMD Plus LFI at the Mahidol Oxford Tropical Medicine Research Unit, before and after concentrating	76
Table 4	Summary of the patient samples and results of paired serum and urine samples tested on the AMD Plus LFI at the University of Nevada, Reno	77

Chapter 4: Development of a lateral flow immunoassay for the detection of Ebola virus soluble glycoprotein

Table 1	Summary of subclass and immunization strategy for the library of seventeen monoclonal antibodies reactive to recombinant EBOV sGP isolated in this study	103
Table 2	Affinity and kinetics analysis of EBOV sGP mAbs by surface plasmon resonance	104

List of Figures

Chapter 1: Introduction

Figure 1	IgG antibody schematic	19
Figure 2	Lateral flow immunoassay (LFI) diagram	20
Figure 3	Variations of antibody binding in an enzyme-linked immunosorbent assay (ELISA)	21

Chapter 2: Magnetic immunoprecipitation for concentrating *Burkholderia pseudomallei* capsular polysaccharide

Figure 1	Schematic of magnetic immunoprecipitation testing protocol	40
Figure 2	Testing of various sample volumes showed an increase in analytical sensitivity when using magnetic particles with larger volumes at the same concentration	41
Figure 3	Capsular polysaccharide at various concentrations was spiked into 10 mL samples of pooled normal human urine and the limit of detection of CPS was determined to be ≤ 1 pg/mL	42
Figure 4	Images of AMD Plus LFI results from testing the human melioidosis samples obtained from Menzies School of Health Research	43
Figure 5	Images of AMD Plus LFI results from testing the human melioidosis samples obtained from Lao-Oxford-Mahost Hospital-Wellcome Trust Research	44
Figure S1	Optimization of the amount of mAb 4C4 conjugated to Invitrogen Dynabeads M-270 Epoxy	47
Figure S2	Optimization of the length of the acid incubation for the magnetic particle protocol	48

Chapter 3: Passive concentration of *Burkholderia pseudomallei* capsular polysaccharide from melioidosis urine samples for the enhanced detection on the Active Melioidosis *Detect*™ Plus lateral flow immunoassay

Figure 1	Images of AMD Plus LFIs showing results when testing samples pre- and post-concentration	79

Figure S1 Image of Vivapore BJP-5/30 concentrators used for concentrating urine samples from melioidosis patients 80

Figure S2 Image of serum samples tested on the AMD Plus LFI after 15 minutes of run time 81

Chapter 4: Development of a lateral flow immunoassay for the detection of Ebola virus soluble glycoprotein

Figure 1 Reactivity of mAbs to recombinant sGP and gamma-irradiated ZEBOV antigen preparations via Western immunoblotting 105

Figure 2 Optimized recombinant sGP antigen-capture ELISA limit of detection 106

Figure 3 Lateral flow immunoassay prototype tested with recombinant sGP spiked into chase buffer at various concentrations 107

Figure 4 Testing of 2HG12 (capture) and 2HG5 (detection) LFI prototype with gamma-irradiated ZEBOV infected Vero E6 cell lysate 108

CHAPTER 1

Introduction

1.1 Overview

The following chapters outline the development of diagnostic immunoassays for the detection of two pathogenic Tier 1 select agents, the bacteria *Burkholderia pseudomallei* and Ebola virus (EBOV). The diagnostics discussed for each pathogen are at different stages of development and the research conducted here can be separated into two distinguishable parts:

I. Diagnostic measures for *B. pseudomallei* (Chapters 2 and 3)

II. Diagnostic measures for EBOV (Chapter 4)

In chapter 1, a general overview of each pathogen and disease is provided, along with information regarding antibodies and immunological assays. Chapters 2 and 3 focus on the detection of *B. pseudomallei* capsular polysaccharide (CPS). These chapters will cover the approaches taken to enrich melioidosis patient urine samples for CPS to increase the positivity rate on a lateral flow immunoassay (LFI). Two approaches are assessed and validated using urine samples from melioidosis confirmed patients. Chapter 4 focuses on the development of a novel LFI prototype for the detection of EBOV soluble glycoprotein (sGP). Finally, an overall conclusion will be provided in chapter 5.

1.2 *Burkholderia pseudomallei* and melioidosis

Burkholderia pseudomallei is the etiological agent of a deadly disease called melioidosis. This motile, oxidase-positive, aerobic Gram-negative bacterium was first described in 1911 at the Rangoon General Hospital in Burma by Alfred Whitmore and C.S. Krishnaswami [1]. The first reported case was a patient who was experiencing a high fever that lasted seven days and several abscesses at the site of morphine injections. The infection was initially diagnosed as glanders, a disease caused by near-neighbor *Burkholderia mallei*, at the time *Bacillus mallei*. Further analysis of the bacillus isolated from the patient postmortem was identified to not be *B. mallei* through clinical and microbiological investigation. Specifically, the bacillus isolated from this patient was motile, whereas *B. mallei* is nonmotile, and the patient was not known to have close contact with horses [2]. From the culture and pathological findings, Whitmore proposed the name *B. pseudomallei* for the bacteria as a result of the glanders-like manifestations [3].

Following its identification, the disease was called Whitmore's disease until it was renamed in 1921 by Stanton and Fletcher who called it melioidosis from the Greek "melis" (distemper of assess) and "eidos" (resemblance) [4]. Up until 1992 when it was formally named *Burkholderia pseudomallei*, the bacteria causing melioidosis had been referred to as many names including *Bacillus pseudomallei*, *Bacillus whitmorii* (or *Bacille de Whitmore*), *Malleomyces pseudomallei*, and *Pseudomonas pseudomallei* [5, 6].

B. pseudomallei is categorized as a Category B select agent by the Centers for Disease Control (CDC) for its catastrophic potential [7]. There is a high risk of its deliberate use as a bioterrorism agent due to its overall ease of spread, high virulence, and general lack of

countermeasures, however, no accounts of malicious dissemination of *B. pseudomallei* have been documented.

Geographic distribution and incidence

B. pseudomallei is primarily endemic in 45 countries across Southeast Asia and northern Australia, corresponding to the tropical latitudes between 20°N and 20°S [6, 8-10]. As a natural saprophyte, this organism can be cultured from soil, fresh water, and rice paddies [11]. *B. pseudomallei* can be found through sampling of the surface soil, though it is far more common to be found in the rhizosphere and surface groundwater [12]. The bacterium is also known to be able to survive in extreme conditions, including surviving in distilled water for sixteen years, but favors areas with high rainfall and soil that has been modified by humans for farming [13, 14].

In 2015, a model proposed by Limmathurotsakul *et al.* estimated the global burden of melioidosis to be 165,000 cases per year worldwide, with a case fatality rate of approximated 54% resulting in 89,000 deaths [15]. This study also suggested that this disease is severely underreported not only in countries with known endemicity, but also in 34 countries where the disease has never been reported but is most likely endemic due to the favorable conditions for this bacterium to thrive in [15]. Multiple countries where *B. pseudomallei* is absent contain favorable conditions for the establishment of the bacteria, including multiple regions in the United States. There have been numerous cases of melioidosis in the United States, including cases due to imported goods and animals, as well as cases where the origin of exposure has yet to be identified [16-19]. Most recently there was a multistate outbreak that was a result of imported aroma therapy goods in which four people became infected and two people died [18].

Transmission and virulence

Transmission of *B. pseudomallei* to humans most commonly occurs through direct contact with contaminated soil or water [20]. The routes of infection include percutaneous inoculation, ingestion, and inhalation of the bacteria [21]. Diabetes mellitus is the most common risk factor for a melioidosis infection, with greater than 50% of all patients worldwide having this metabolic disease [22, 23]. Other predisposing health risk factors include kidney disease, being of the male sex, thalassemia, liver disease, and high alcohol intake [6, 23, 24]. Farmers becoming infected with that bacteria via dermal abrasions while working in rice paddies is a common occurrence in Southeast Asia [25]. Regardless of the numerous predispositions making one more likely to acquire a *B. pseudomallei* infection, over 80% of pediatric patients, and approximately 20% of adult patients do not have any underlying risk factors [22, 26]. While there are some documented cases of animal to human and human to human cases, these cases are extremely rare and are not a typical route of infection [27, 28].

Clinical features

A melioidosis infection may manifest itself as acute, chronic, or latent. The incubation period can vary quite broadly, from 2-3 days up to years as is seen in latent infections [6, 29-31]. However, the average incubation period for an acute infection is nine days [31]. The clinical manifestations of the disease often present as nonspecific, flu-like symptoms making a diagnosis based purely on symptomology challenging. Other typical symptoms include pneumonia, abscesses, and generalized organ failure. These broad symptoms often result in an initial misdiagnosis. Furthermore, some patients develop cavities in the upper lobes of the lung which gives an appearance of tuberculosis on chest films [32]. The described lack of identifiable symptoms has earned *B. pseudomallei* the name, “the great

mimicker” [33]. The symptom presentation is often dependent on the route of infection, for example skin ulceration is common following a cutaneous infection and pneumonia in infections resulting from inhalation [34-36]. Overall, bacteremia occurs in 40-60% of all cases, pneumonia occurs in about 50% of cases, and septic shock occurs in about 20% of cases [37]. Chronic melioidosis constitutes 10% of all cases and is defined as persistent symptoms lasting longer than two months [38]. A latent infection can be reactivated as a result of immunosuppression following an asymptomatic infection in which the pathogen was not effectively cleared, and this form of infection is estimated to cause approximately 5% of melioidosis infections [38].

Diagnosis

Isolation of the bacterium through the culturing of bodily fluids remains the gold standard for diagnosing melioidosis for the lack of a better alternative. This method can take up to seven days to determine a result and although specificity is 100%, the sensitivity is approximately 60% [39]. The purportedly low sensitivity of this diagnostic method can be attributed to the low bacterial load that is seen in many patients; the average being 1 colony forming unit per milliliter (CFU/mL) in blood [40, 41]. This method also requires access to the appropriate selective media and trained laboratory personnel [42]. Other diagnostic methods for melioidosis include polymerase chain reaction (PCR), serological assays, and other immunoassays that rely on the identification of *B. pseudomallei* specific antigens [43-48]. PCR is not often used in certain endemic areas given the cost and limited sensitivity [49]. Indirect hemagglutination assays (IHAs) are a standard in serological assays to diagnose an infection through the detection of host antibodies reactive to *B. pseudomallei* antigens, including capsular polysaccharide (CPS) and O-polysaccharide (OPS), but the sensitivity and specificity are low [50]. Serological enzyme-linked

immunosorbent assays (ELISAs) have been developed for the detection of OPS and hemolysin co-regulated protein 1 (Hcp1) which show great sensitivity but given the nature of endemicity of this bacterium, serological assays are difficult to standardize in certain populations [51, 52]. The identification of Hcp1 as a potentially better serodiagnostic target led to the development of an immunochromatography test (ICT) for the detection of Hcp1 antibodies [53]. While it shows great promise, more studies need to be conducted to implement this is an alternative diagnostic method.

Alternative rapid diagnostic methods for melioidosis have been developed, including immunofluorescence assays (IFAs) and lateral flow immunoassays (LFIs) [43, 44, 54]. These assays have been developed for the direct detection of *B. pseudomallei*, its antigens, or patient antibodies reactive to the bacteria or its antigens. An IFA was developed for the detection of the bacteria using CPS specific antibodies and while the specificity is high, the sensitivity is low [44]. A LFI has been developed in our laboratory in collaboration with InBios International, Inc. for the rapid detection of *B. pseudomallei* in fifteen minutes [43]. The LFI has a high specificity, but sensitivity varies [55, 56]. The analytical sensitivity for CPS is reported at 200 pg/mL, however, the clinical sensitivity can be low depending on the sample type [43, 55]. There are many diagnostic methods being explored for the rapid diagnosis of melioidosis, but further research and evaluation needs to be conducted in order to achieve substantially better diagnostic performance over culturing of patient samples.

Treatment

Identification of *B. pseudomallei* infections is essential as the bacterium is intrinsically resistant to many front-line antibiotics, including penicillin, ampicillin, gentamicin, and

others [57, 58]. The case fatality rate (CFR) for melioidosis without administration of the appropriate antibiotics has been reported as high as 70%, and with the appropriate antibiotics the CFR can still be up to 45% [15]. Treatment for melioidosis consists of two phases: IV and oral [59]. The first phase of treatment consists of IV therapy which focuses on treating septicemia. The second phase of treatment consists of oral therapy which focuses on eradication of the bacteria. Phase one of treatment typically consists of ceftazidime or meropenem for 10-14 days, with the latter being preferred for severe cases of melioidosis [60]. Phase two consists of at least three months of oral therapy, trimethoprim/sulfamethoxazole (co-trimoxazole) as the preferred drug, for the eradication of the bacteria [60]. Non-compliance with the recommended three month regime is often observed due to limited access to the antibiotics, cost, and side-effects of the drugs [60]. A relapse and/or latent reactivation of the infection can occur if the bacteria is not eradicated. Co-trimoxazole can also be administered as a post-exposure prophylaxis for melioidosis for a duration of twenty-one days [60].

1.3 Ebola virus and Ebola Virus Disease

Ebola virus disease (EVD) is a deadly disease caused by four species of viruses within the genus *Ebolavirus*. Specifically, the species that have been identified as being able to cause this disease in humans are *Zaire ebolavirus* (ZEBOV), *Sudan ebolavirus* (SUDV), *Bundibugyo ebolavirus* (BDBV), and *Taï Forest ebolavirus* (TAFV) [61]. There are two other species within this genus, *Reston ebolavirus* (RESTV) and *Bombali ebolavirus* (BOMV), but they have not been identified as causing disease in humans. RESTV is known to cause disease in nonhuman primates and pigs. BOMV was identified in 2018 in bats, but it is unknown if it can cause disease in humans or animals.

The first recorded cases of EVD occurred in 1976 in southern Sudan [62]. This outbreak resulted in 284 cases and had a CFR of 53%. However, the virus was not identified until the second outbreak occurred in northern Zaire, which is now known as the Democratic Republic of the Congo, later in the same year [63]. In all, this second outbreak resulted in 318 cases and had a CFR of 88%, causing 280 deaths. The cause of the initial outbreak was thought to be Marburg virus, a near-neighbor, however, it was discovered to be a new virus related to the genus *Marburgvirus*. This novel virus was named Ebola virus (EBOV) after the Ebola River that is found in the Democratic Republic of the Congo. While both of these outbreaks were caused by a species of *Ebolavirus*, it was not discovered until years later that each outbreak was in fact caused by a different species, SUDV and ZEBOV respectively [64].

EBOV is categorized as a Category A select agent by the CDC as it poses a severe threat to human health [7]. This virus has a high CFR, low infectious dose, and can easily be disseminated from person to person, making it a potentially malicious bioweapon.

Geographic distribution and incidence

To date over 33,000 cases of EVD have been reported resulting in over 14,000 deaths. Up until 2013, SUDV was responsible for the largest outbreak of Ebola virus [65]. However, following the 2013-2016 West African Epidemic, ZEBOV is now responsible for the majority of all EVD cases. In this outbreak, which is the largest recorded outbreak in history, there were 28,646 reported cases and 11,323 deaths spanning multiple countries [61, 66]. All human outbreaks have originated in West and Central Africa, within 10° of the equator [67]. While cases of EVD have been reported outside of this region, these cases have been a result of traveling after becoming infected, being infected while treating an EVD patient, or a laboratory acquired infection [61]. There have been RESTV outbreaks in animals in both the Philippines and the United States. In the Philippines, there have been a total of three outbreaks, two in nonhuman primates and one in pigs, [68-70]. Two of these outbreaks, one with pigs and one with nonhuman primates, resulted in the virus being transmitted to humans, however the humans remained asymptomatic and showed no signs of illness. The RESTV outbreak that occurred in cynomolgus monkeys in a facility in Reston, Virginia, was determined to be caused by an imported monkey from the Philippines [71].

Transmission and virulence

EBOV is transmitted through the direct contact with an infected person or contaminated bodily fluids, though it may also be able to be transmitted through aerosols [72]. Infected patients can harbor the virus in their blood, urine, semen, saliva, and breast milk and contact by a healthy individual with any of these bodily fluids can transmit the virus and cause disease. While risk factors are not well-defined, it appears that women as caregivers may be at a higher risk of infection, as well as children particularly under the

age of 5 [72, 73]. Pregnant women who become infected with Ebola virus have a high risk of miscarriage and EBOV transplacental transmission, though rare, has been reported [74, 75]. The natural host reservoir of the virus is still unknown, though it is suspected to be fruit bats [76]. The infectious dose for Ebola virus is low with reports indicating it could be as low as 10 virions [77]. Ebola viruses are highly virulent with the mean time of death just 7-8 days from the onset of symptoms [32]. Outbreaks on record have had a CFR of 25-90%, with an average of roughly 45% [61].

Clinical features

The average incubation period of EBOV is 2-21 days, with a mean of 4-10 days, which is followed by the abrupt onset of an acute hemorrhagic fever [74]. EVD patients are not considered infectious until the initial onset of symptoms [66]. Initial symptoms of the disease are nonspecific and include fever, chills, malaise, and myalgia. These symptoms can often be the cause of a misdiagnosis [78]. As the disease progresses, more symptoms appear indicating multisystem involvement. The next set of symptoms that typically appear are gastrointestinal including nausea, vomiting, and diarrhea. At about 6-10 days post symptom onset, viremia is detectable, and patients typically suffer from fever, hypotension, and dehydration [72]. In the terminal phase of the hemorrhagic fever, multiorgan failure may be observed as well as internal and external bleeding [72].

Diagnosis and treatment

The current gold standard for diagnosing EVD is polymerase chain reaction (PCR), though typically an initial diagnosis is made based on clinical assessment and a history of travel to a known endemic area [74, 79]. However, diagnosis is difficult based on this method as there are many acute febrile causing diseases that are common in the Ebola endemic

areas including malaria and typhoid fever among others. When EVD is suspected, laboratory diagnosis is made through centralized testing centers where PCR is performed, where the detection of Ebola virus nucleic acid is made from a blood sample. In some cases, an antigen detection enzyme-linked immunosorbent assay (ELISA) is performed to detect the presence of EBOV antigens, or a serological ELISA may be performed to detect antibodies for EBOV antigens [80, 81]. These two assays, PCR and ELISA, can take hours to perform, require trained personnel, and access to specialized laboratory equipment. During the West African Epidemic, test results were delayed for days, which had an impact on successfully isolating patients to reduce the spread of the virus [72]. A rapid point-of-care (POC) lateral flow immunoassay (LFI), called ReEBOV Antigen Rapid Test, was given emergency use authorization (EUA) for the rapid detection of EVD through detection of EBOV viral matrix protein VP40. This test has since had its EUA revoked, though there are currently other LFIs that still have EUA.

There are currently two U.S. Food and Drug Administration (FDA) approved therapeutic treatment options for EVD, Inmazeb and Ebanga, though their efficacies are only 65% [82]. These two treatments have only been evaluated for their efficacy against ZEBOV. Both treatments consist of monoclonal antibodies that are used to inhibit the virus from replicating inside the host [83, 84]. This is accomplished by the antibodies binding to the surface glycoprotein of the virus and preventing entry of the virus into the host cell. Without access to the cellular components within the host cell, the virus is not capable of replication. These treatments can be cost prohibiting to many people in endemic regions and in these cases supportive care including fluids, blood pressure support, managing fever, and reducing vomiting and diarrhea can be performed to improve the chances of survival [85].

Ervebo is the first FDA approved vaccine for EVD [86]. The vaccine is based on the vesicular stomatitis virus which produces ZEBOV glycoprotein (GP) to confer protection against an infection [87]. Once vaccinated, the immune system will illicit an antibody response to ZEBOV GP and these antibodies will prevent the virus from invading host cells similar to the therapeutic treatments. The vaccine has an efficacy of 100%, although that is based on a study looking at up to eighty-four days post vaccination and it has only been evaluated for ZEBOV [88]. It is unknown how long protection is conferred and if this vaccine can protect against other species of EBOV.

1.4 Antibodies

The human immune system is comprised of two main responses: the innate immune response and the adaptive immune response [89]. The innate immune response is fast and will occur rapidly following an infection. The adaptive immune system can take days to develop as cells from the adaptive immune response can recognize specific antigens from a pathogen after a maturation process. During the adaptive immune response, naïve lymphocytes encounter an antigen, become activated, and differentiate into effector lymphocytes [90]. There are two types of lymphocytes, B lymphocytes (B cells) and T lymphocytes (T cells). Once a specific antigen binds to a B-cell antigen receptor (BCR), proliferation occurs and they further differentiate into plasma cells, which is the effector form of B cells [89]. These effector B cells produce immunoglobulins (Ig), a receptor that is specific for the antigen that caused the naïve lymphocyte to differentiate. These Igs can also be secreted from the cell as an antibody, however the antibody varies slightly in that it does not contain a C-terminal hydrophobic region that is used to anchor the BCR to the membrane of the B cell [90, 91]. Instead, the antibody contains a hydrophilic region that promotes secretion. The role of an antibody during the adaptive immune response is two-fold: bind to its target and then recruit other cells or molecules to destroy the target.

The overall structure of the 150 kDa antibody molecule is roughly a Y shape that is comprised of two different kinds of polypeptide chains, the heavy chain of approximately 50 kDa and the light chain of approximately 25 kDa [92]. Each antibody molecule is comprised of two identical heavy chains and two identical light chains that are linked together by disulfide bonds (Figure 1). The antibody can be further differentiated into two distinct regions, the variable region and the constant region [93]. The variable region consists of two domains, one from the heavy chain (V_H) and one from the light chain (V_L).

The constant region consists of three domains from the heavy chain (C_H1, C_H2, C_H3) and one domain from the light chain (C_L) for an IgG antibody (Figure 1). Each region has its own function. The variable region is responsible for antigen binding and recognition and the constant region is responsible for interacting with effector cells and molecules [94]. There are five major classes, or isotypes, of Igs: IgG, IgM, IgA, IgD, IgE, which are determined by the constant region of the heavy chain [94]. IgG is the most abundant isotype found in humans and is the most extensively studied isotype [92]. IgG has several different subclasses. In humans they are IgG1, 2, 3, and 4, but in mice they are IgG1, 2a, 2b, and 3 [95]. The highly specific nature of antibodies is essential to their role in the immune system and this capability has implications in research applications, therapeutics, and diagnostics.

1.5 Diagnostic Immunoassays

Immunoassays are methods used in research and diagnostics that exploit the basic nature of the binding affinity of an antibody to its target (analyte) [96]. In these assays, the analyte is bound to the antibody to form an immune complex. The formation of these immune complexes is evaluated through some form of antibody labelling and/or chemical detection reagents to aid in visualization, either with the naked eye or from specialized equipment. These forms of labeling can vary depending on the type of immunoassay platform being run, including fluorescent tags, enzymes, and nanoparticles [97]. When immunoassays are developed for diagnostic purposes, they typically focus on the detection of pathogen specific antigens or host antibodies that are produced in response to these antigens.

Lateral flow immunoassay

Lateral flow immunoassays (LFI) are one form of a diagnostic immunoassay that is commonly used at the POC [98]. In fact, LFIs are commonly used at home and include home pregnancy tests and COVID-19 antigen tests [99, 100]. Some advantages of LFIs are that they are rapid, typically providing a result in less than 20 minutes, low cost, do not require specialized equipment, and little training is needed [101]. This is beneficial for resource poor areas, such as the areas where melioidosis and EVD are endemic.

The LFI platform utilizes antibodies and a label to detect a specific biomarker for a disease or other condition. The basic overall construction of an antigen detection LFI can be found in Figure 2. In short, a conjugate pad and a wicking pad overlap a nitrocellulose membrane and are mounted on a backing card. The conjugate pad contains an antibody that is reactive to the biomarker of interest and is labeled with colloidal gold nanoparticles to visualize any binding events. The nitrocellulose membrane contains two lines of

immobilized antibodies. The first line is immobilized with an antibody, or antibodies, that are specific to the biomarker of interest to form the test line. Visualization of the test line will indicate if the biomarker is present in a sample and therefore a indicate a positive diagnosis. A second line of antibody is immobilized to form the control line that is used to validate the test. If the control line is not visible, the test result is invalid. A sample consisting of blood, urine, or other matrix is applied to the conjugate pad and if the biomarker is present, the gold labeled antibody will bind to it. The wicking pad facilitates capillary action which pulls the sample into the nitrocellulose membrane. Any complexes that consist of the biomarker and gold labeled antibody will be captured at the test line in the form of “sandwich binding”, resulting in the colorization of the test line [102]. Any labeled antibody that is not immobilized at the test line will travel further up the nitrocellulose membrane and can be captured at the control line. There are other forms of LFIs including serological LFIs for the detection of antibodies as well as competitive LFIs where the visualization of the test line indicates a negative result [103, 104].

Enzyme-linked immunosorbent assay

ELISAs are another type of immunoassay that can utilize multiple orientations of immune complexes to detect a variety of biomarkers (Figure 3) [105, 106]. As a diagnostic platform, ELISAs can be used to detect an antigen through the direct, indirect, or antigen-capture format. Serological ELISAs can also be performed to determine if a patient sample contains antibodies reactive to a specific antigen produced by a specific pathogen. ELISAs are a sensitive and commonly used to diagnose infectious diseases, however, they do require some training, access to laboratory equipment, and can take several hours to produce a result [107]. Regardless, ELISAs are a great diagnostic tool and have many research applications as well.

ELISAs are typically performed in a microtiter well. In a direct ELISA, the target antigen is coated in the well. This antigen is identified following an incubation with a primary antibody that labeled, usually with horseradish peroxidase (HRP), which will bind to the antigen. In the case of HRP labeled antibody, a colorimetric change occurs when tetramethylbenzidine substrate is added to the well [108]. An indirect ELISA is similar to a direct ELISA but requires an extra step to introduce the HRP labeled antibody. As before, a well is coated with an antigen and incubated with an unlabeled primary antibody, e.g., a patient sample that may contain the antibody of interest. However, this binding would not be able to be visualized, so an incubation with an HRP labeled secondary antibody, that binds the primary antibody, is performed prior to introducing the substrate. Antigen-capture ELISAs, also referred to as a “sandwich” ELISA, take a slightly different approach. For example, an unlabeled antibody is used to coat the well and then a sample is added. If the antigen is present, it will bind to the antibody coating the well. This will enable the detection HRP antibody to be captured in the well by binding to the antigen and in doing so form a “sandwich”. Once substrate is added, there will be a colorimetric change. If the antigen is not present in the sample, the secondary antibody will not be captured and when substrate is added, there will be no colorimetric change as there will not be any HRP for the substrate to interact with.

1.6 Figures

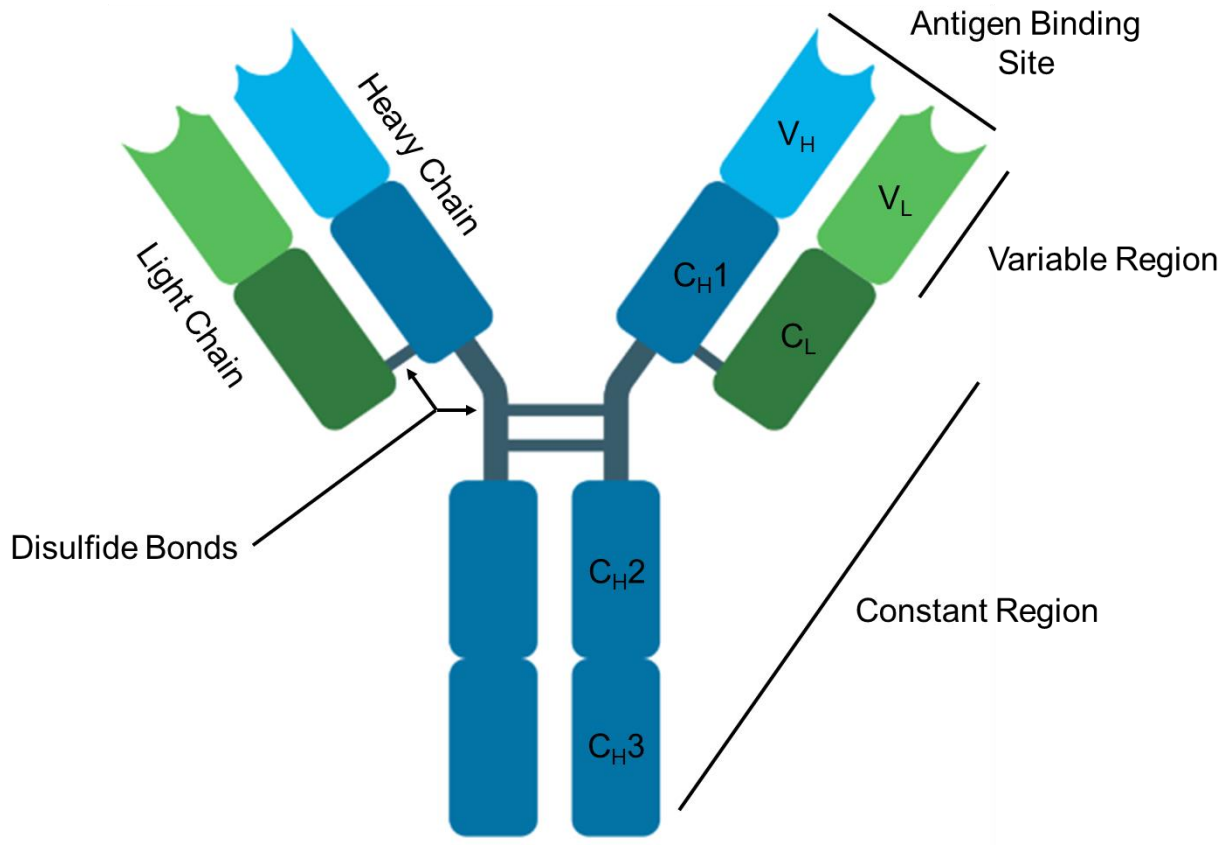

Figure 1. IgG antibody schematic. The IgG antibody molecule is comprised of two distinct polypeptide chains, heavy and light. Each antibody is made of two heavy and two light chains linked together by disulfide bonds. The light chain contains a variable domain (V_L) and a constant domain (V_H). The heavy chain contains one variable domain and three constant domains. The variable region contains both variable domains (V_L and V_H) and the constant region contains all four constant domains (C_L, C_H1, C_H2, and C_H3). Created with BioRender.com.

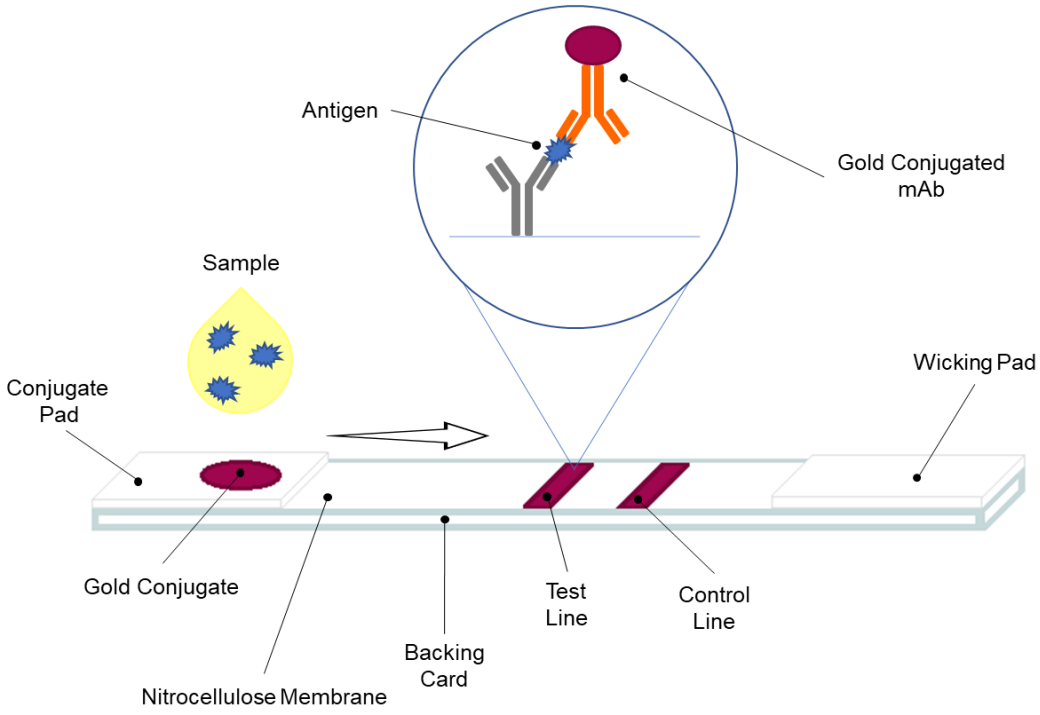

Figure 2. Lateral flow immunoassay (LFI) diagram. The LFI is comprised of overlapping pads and membranes, each with their own function. The conjugate pad contains labeled antibody to interact with the sample once it is applied. The wicking pad draws the sample up the nitrocellulose membrane where it will encounter antibodies that function as a test line and another antibody that functions as a control line. Visualization of the test line indicates a positive result and visualization of the control line indicates that the test functioned properly. Created with BioRender.com.

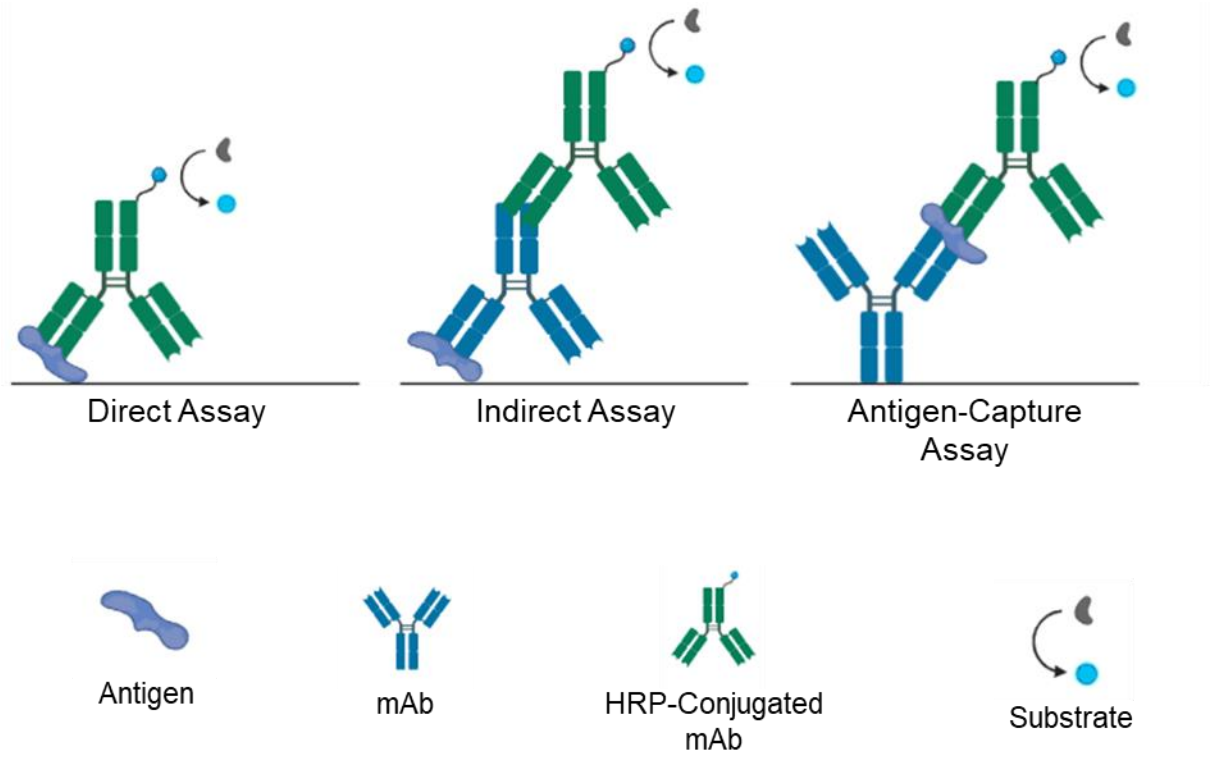

Figure 3. Variations of antibody binding in an enzyme-linked immunosorbent assay (ELISA). Direct ELISAs utilize HRP-conjugated antibodies to bind to a target and substrate is added for a colorimetric visualization. Indirect ELISAs use a primary antibody to bind to the target and a separate HRP-conjugated secondary antibody for the colorimetric visualization. Antigen-capture ELISAs use one antibody to capture the antigen from a sample and a HRP-conjugated detection antibody to bind to the captured antigen and allow for the colorimetric visualization. Created with BioRender.com.

CHAPTER 2

Magnetic immunoprecipitation to concentrate *Burkholderia pseudomallei* capsular polysaccharide

Heather R. Green[1], Chelsea C. Chung[1], Jacob T. Sorensen[1], Derrick Hau[1], Emily E. Hannah[1], Haley L. DeMers[1], Sujata G. Pandit[1], Peter N. Thorkildson[1], Marcellene A. Gates-Hollingsworth[1], Mary N. Burtnick[1], Paul J. Brett[1], Celeste Woerle[2], Mark Mayo[2], Bart J. Currie[2], Kate L. Woods[3], Manophab Luangraj[3], Latsaniphone Boutthasavong[3], Viengmon Davong[3], David A. B. Dance[3,4] and David P. AuCoin[1]

Author Affiliates: [1]Department of Microbiology and Immunology, University of Nevada, Reno School of Medicine

[2]Menzies School of Health Research, Royal Darwin Hospital Campus, Casuarina, Australia

[3]Lao-Oxford-Mahosot Hospital-Welcome Trust Research Unit, Microbiology Laboratory Mahosot Hospital, Vientiane, Lao PDR

[4]Centre for Tropical Medicine and Global Health, University of Oxford, UK, [5]DxDiscovery, Inc. Reno, NV

*Corresponding author

Email: daucoin@med.unr.edu

2.1 Abstract

Burkholderia pseudomallei is a soil-dwelling, Gram-negative bacterium that is ubiquitously found in tropical regions. It is the causative agent of melioidosis, a life-threatening illness that is prominent in Southeast Asia and northern Australia. Melioidosis is difficult to diagnose as the symptoms are typically non-specific contributing to an estimated 89,000 deaths per year. In Southeast Asia, mortality rates are reported to be 40-50%, even with the most effective antibiotics. The current gold standard to diagnose melioidosis is blood culture, however, this process takes up to seven days to perform and only identifies roughly 50% of infections. A more rapid diagnostic is needed to quickly identify infected patients and potentially reduce the morbidity and mortality associated with melioidosis. A lateral flow immunoassay (LFI) has been developed to detect the capsular polysaccharide (CPS) of *B. pseudomallei*, which is detectable at low concentrations in blood and urine during various stages of infection. This rapid diagnostic platform is low-cost, making it ideal for resource-limited areas. The concentration of CPS in patients can vary by orders of magnitude, from sub-picograms per milliliter to micrograms per milliliter, so a melioidosis antigen-detection assay needs to have a large dynamic range to detect clinically relevant levels of CPS in patient samples. A novel protocol utilizing magnetic particles and acid-base elution-neutralization has been developed to concentrate CPS out of larger sample volumes prior to being run on the LFI. Utilizing this protocol, we have shown an enhanced detection of purified CPS as well as the ability to increase the test line intensity of human melioidosis urine samples when compared to the standard LFI testing method.

2.2 Background

Burkholderia pseudomallei is a highly pathogenic environmental bacterium and the causative agent of melioidosis [109]. Clinical manifestation of melioidosis may present in an acute form following an incubation of one day to three weeks, or in a latent form, which may not present for decades after contracting the bacterium [110]. Clinical manifestations of this disease are many, including organ abscesses, sepsis, and mild infection of the skin, with the route of infection contributing to the clinical symptomology [110, 111]. While *B. pseudomallei* most commonly causes severe disease in people with underlying risk factors such as diabetes, it can also infect healthy individuals [112-114]. Global distribution models of melioidosis estimate there are approximately 165,000 cases per year resulting in 89,000 deaths, though the disease is often underreported [15]. The underreporting can be contributed to the lack of knowledge surrounding the disease and the bacterium. In fact, melioidosis is not listed as a neglected tropical disease despite contributing to more fatalities per year than other diseases that are recognized on the list. *B. pseudomallei* is also categorized as a Tier 1 Select Agent by the Centers for Disease Control and Prevention given the ability of this bacteria to be aerosolized, lacks a vaccine, and confounding clinical manifestations further contributes to this bacterium's threat to public health [37].

The current gold standard for diagnosing melioidosis relies on culturing and isolating *B. pseudomallei* from clinical samples, usually blood. All other diagnostics are compared to culture [115]. Culture has its drawbacks, it has been shown to be an imperfect gold standard and time to result can take as long as seven days [115, 116]. The extended diagnosis time is of particular concern as *B. pseudomallei* is intrinsically resistant to many

broad-spectrum antibiotics that are commonly used to treat other Gram-negative infections [60, 117]. Melioidosis requires extensive therapeutic regimens, including IV therapy for up to 12 weeks and oral therapy for up to six months [118]. Consequently, a rapid diagnosis is imperative to ensure the proper antibiotics are administered, lessening the burden of melioidosis.

The lateral flow immunoassay (LFI) test is a rapid diagnostic tool that can be used to detect specific biomarkers in a sample utilizing antibody-based technology [119]. This antigen-capture platform works by incorporating antibodies into a membrane-based assay, where high affinity antibodies bind target biomarkers at a test-line, indicating a positive result. Some of the many advantages of an LFI include point-of-care (POC) usability, that is they can be performed without having to be transferred to a clinical lab, are low cost, and are easy to use [120]. These advantages illustrate the benefit that an LFI would provide to resource limited areas, such as Southeast Asia, where melioidosis is endemic.

The capsular polysaccharide (CPS) of *B. pseudomallei* has been previously identified as an encouraging clinical diagnostic biomarker for melioidosis [49]. The detection of CPS at low concentrations is imperative as early administration of appropriate antibiotics significantly impacts the prognosis of the patient [111, 121]. In response, the Active Melioidosis *Detect*™ Lateral Flow Immunoassay (AMD LFI) was developed by InBios International Inc. (Seattle, WA, USA) and our laboratory as a POC diagnostic tool to detect CPS within patient samples [43]. The AMD LFI uses a monoclonal antibody, 4C4, that is reactive to *B. pseudomallei* CPS [122]. The limit of detection (LOD) or analytical sensitivity of CPS for the AMD LFI is roughly 200 pg/mL [43]. During the timeline of this project,

InBios re-optimized the AMD LFI to make the AMD™ Plus LFI. The AMD Plus LFI has an estimated limit of detection between 80-160 pg/mL based on personal communication and is housed in a cassette. The LOD of the AMD LFI is impressive, especially for this diagnostic platform. The LOD achieved by the AMD LFI may be attributed to the structure of CPS, which is a multivalent polysaccharide with a repeating homopolymer structure [123]. The repeating epitope contained within CPS presumably allows multiple detection antibodies to bind a single CPS molecule, thus enhancing the LOD of the LFI.

Urine is a non-invasive sample and large volumes can be collected easier than serum samples. Given these advantages, urine appears to be the best matrix for diagnosing melioidosis for this LFI diagnostic platform. Furthermore, CPS quantification in both urine and serum indicate that urine may contain more CPS than serum. Experiments conducted in our laboratory have indicated that CPS can be present over several orders of magnitude in melioidosis patient urine and serum samples: ranging from sub-picograms to micrograms per milliliter in each matrix [124]. This trend was identified over two separate studies involving two separate cohorts of samples. One cohort of samples was from Menzies School of Health and research located in Darwin, Australia and the other sample cohort was from Lao-Oxford-Mahosot Hospital-Wellcome Trust Research Unit located in Vientiane; both are areas that have been defined as high-risk zones for melioidosis [15].

Despite the potential for large sample volumes, particularly for urine, the design of an LFI is such that the device can only accommodate a limited volume. The AMD LFI is compatible with 150 µL of sample, which limits the amount of CPS available for detection. To overcome this limitation, we have developed a POC method that combines magnetic

immunoprecipitation to concentrate CPS from sample volumes ranging from 1-10 mLs prior to running the sample on the AMD LFI, thereby enhancing the detectable amount of CPS in the limited sample volume that can be run on the LFI. This improvement renders the AMD Plus LFI a rapid diagnostic test for melioidosis that is sensitive enough to detect CPS within samples at the sub-picogram per milliliter level.

2.3 Methods

Ethics Statement

Studies on human subjects were approved by the University of Nevada, Reno Institutional Review Board (IRB).

Conjugation of 4C4 to Invitrogen Dynabeads M-270 Epoxy

CPS reactive mAb 4C4 was covalently conjugated to Invitrogen Dynabeads M-270 Epoxy (ThermoFisher Scientific, Waltham, MA) per the protocol provided with the product, with slight modifications. Briefly, Dynabeads were resuspended and washed in 0.1 M sodium phosphate buffer, pH 7.4, and 3M ammonium sulfate. 500 µg of 4C4 was then coupled to 2.5 mg of the Dynabeads in an overnight incubation. The conjugate was washed in PBS with 1% BSA and 0.05% Tween™ 20, pH 7.4, and resuspended in PBS with 0.1% BSA, pH 7.4. Next, the conjugate is subjected to an acid treatment of 200 µL of 1 M Glycine-HCl, pH 1.3. Finally, the conjugate was washed again in PBS with 1% BSA and 0.05% Tween™ 20, pH 7.4, and resuspended in PBS with 0.1% BSA, pH 7.4.

Protocol for Magnetic Immunoprecipitation

The basic protocol is outlined in Figure 1. CPS, purified by the Brett laboratory as previously described [125], was spiked into either PBS or a pooled normal human urine sample. Dynabead-4C4 conjugate was added to the sample at a ratio of 1:20. The sample was then incubated at room temperature for 10 minutes with rotation. Next, the CPS and Dynabead complex was separated using a DynaMag magnet (ThermoFisher Scientific,

Waltham, MA) for 2 minutes. The supernatant was removed and discarded. The sample was then removed from the magnet and the pellet was resuspended in 40 µL of 1 M Glycine-HCl, pH 1.3. The sample was incubated at room temperature for 30 minutes and then placed back on the magnet for 2 minutes. The supernatant, containing the eluted CPS, was removed and collected into a new tube containing 30 µL of 1 M Tris, pH 13.0. The neutralized sample was then immediately applied to the sample pad of the AMD LFI (InBios International Inc., Seattle, WA). For 10 mL samples, the following modifications were employed: initial magnet step was increased to 5 minutes and the acid incubation step was 20 minutes. 5 mL samples followed the exact same protocol as the 10 mL sample protocol.

LFI Testing – PBS and Normal Human Urine

Various sample volumes of PBS or pooled normal human urine were spiked with various amounts of CPS. The samples then underwent the magnetic immunoprecipitation protocol as described above. After neutralization, the samples are applied directly to the sample pad of the LFI. Two drops of Chase Buffer A, provided by InBios International Inc. with the AMD LFI kit, was added to a microtiter well, and the LFI was dipped into the buffer. LFIs were run for 15 minutes and then visually evaluated and read using a Qiagen ESE Quant Reader (Qiagen, Hilden, Germany).

Active Melioidosis Detect Rapid Test (AMD) Lateral Flow Immunoassay (LFI)

Per the manufacturer's recommendation for testing using with the AMD LFI or the AMD Plus LFI, 50 µL of undiluted urine is applied to the sample pad. For the AMD LFI, it is then

immersed in a microtiter well containing two drops of Chase Buffer A. For the AMD Plus LFI, two drops of Chase Buffer A are applied to the sample pad. The results are evaluated once the LFI has run for 15 minutes.

Removal of *B. pseudomallei* Whole Cells from Patient Samples

A panel of human melioidosis patient urine samples were obtained from Menzies School of Health (Menzies) and Research and Lao-Oxford-Mahosot Hospital-Wellcome Trust Research Unit (LOMWRU). These samples were received at the biosafety level 3 and filter sterilized, using a 0.22 µm filter, to clear *B. pseudomallei* from the samples. Two methods were used to verify sterility: culturing the filtrate in liquid media for at least 72 hours and then back plating the liquid media and incubating for 72 hours. Both methods were required to be negative to confirm the filtrate was sterilized. After verifying *B. pseudomallei* whole cells were not present in the filtrate, the samples were downgraded to biosafety level 2 and used for evaluation of CPS via antigen-capture ELISA and testing with the AMD Plus LFI.

Quantitative Antigen-Capture Enzyme-Linked Immunosorbent Assay (ELISA)

An antigen-capture ELISA using mAb 4C4 was performed to quantify CPS in sterile human melioidosis urine samples as previously described [43, 124, 126]. Briefly, 96 well microtiter plates were coated with 100 µL/well of 2.5 µg/mL of 4C4 diluted into PBS and incubated overnight. Following washing and blocking of the plate, one-part sample was diluted with one-part blocking solution (phosphate-buffered saline with 5% skim milk and 0.5% Tween-20) for a 2-fold serial dilution across the plate for a final volume of 100 µL/well. Plates were

incubated for 90 minutes at room temperature. To generate a standard curve, purified *B. pseudomallei* CPS spiked into normal human urine was used starting at 30 ng/mL for a 2-fold serial dilution across the plate. Plates were again washed and then incubated with 100 µL/well of HRP conjugated 4C4 at 0.5 µg/mL for 60 minutes. HRP conjugation of mAb 4C4 was performed using EZ-Link Plus Activated Peroxidase (ThermoFisher Scientific, Grand Island, NY). Plates were washed and then incubated with 100 µL/well tetramethylbenzidine substrate for 30 minutes (SeraCare, Milford, MA). The reaction was stopped with 1M H_3PO_4 (100 µL/well) and the plates were read at optical density 450 nm (OD_{450}). Each sample was analyzed in triplicate.

LFI Testing – Human Melioidosis Patient Urine Samples

Six samples from Menzies School of Health (Menzies) and five samples from Research and Lao-Oxford-Mahosot Hospital-Wellcome Trust Research Unit (LOMWRU) were selected to undergo the magnetic immunoprecipitation protocol. The samples that were received from Menzies underwent the 1 mL protocol as described above and the samples that were received from LOMWRU underwent the 10 mL protocol as described above. As a comparison, the samples were also run on the LFI using standard testing protocol at the same time. LFIs were allowed to run for 15 minutes and then visually evaluated and read using a Qiagen ESE reader (Qiagen, Hilden, Germany) which has an output of optical density (OD).

2.4 Results

Magnetic Immunoprecipitation of CPS

The specificity of the magnetic immunoprecipitation is derived from the conjugation of an antibody reactive to *B. pseudomallei* CPS (4C4) to a magnetic bead. Initial conjugation of the Dynabeads to mAb 4C4 was conducted per the manufacturer's protocol and was further optimized. Increasing the amount of mAb 4C4 conjugated to the Dynabeads provided an increase in the signal intensity of the test line (S1 Fig). Of the concentrations tested, 500 µg of 4C4 conjugated to 2.5 mg resulted in the strongest signal test line intensity. It was also found that prewashing the Dynabead-antibody conjugate with acid prior to testing was ideal to remove any unbound antibody that would otherwise interfere with the detection of CPS.

Additionally, the ratio of conjugate to sample, time required for magnetic separation, the amount of acid and base, and length of the acid incubation period were all optimized for 1 mL and 10 mL testing protocols. Each parameter was evaluated using a standard concentration of CPS at 50 pg/mL and evaluated relative to the other parameters. Changes in protocol that resulted in the highest signal on the AMD LFI, as assessed by the Qiagen ESE reader, were included in the final protocol. An example of validating and selecting a protocol parameter can be found in Supplementary Figure 2.

The optimized protocol was evaluated for its ability to concentrate CPS from larger sample volumes, 1-10 mLs, to overcome the sample volume limitation of the LFI. This was done by running three PBS sample volumes of 150 µL, 1 mL, and 10 mL all at the same

concentration of CPS, 50 pg/mL. The 150 µL sample was run per the manufacturer's recommended testing protocol, while the 1- and 10-mL samples were run after magnetic immunoprecipitation. All samples were run on the AMD LFI and results were evaluated after 15 minutes. Results indicated a stronger test line intensity correspond to a larger sample volume, with the 10 mL sample providing the strongest intensity (Fig 2), suggesting that the conjugated beads are not saturated by the CPS present in the 1 mL volume. The test line intensity observed in Figure 2 indicates a relationship of increasing signal strength with increasing amounts of CPS present in a larger sample, thereby validating this protocol's ability to concentrate CPS out of larger sample volumes.

CPS Limit of Detection in Urine

We next evaluated the analytical sensitivity or limit of detection (LOD) of this sample preparation protocol. CPS was spiked into 10 mL of pooled normal human urine starting at 32 pg/mL and serial diluted down to 0.125 pg/mL. Each dilution was subjected to the magnetic immunoprecipitation protocol and then applied to the AMD™ LFI. Each LFI had a quantitative value assessed by the ESE Quant LFI reader, as well as a qualitative positive or negative reading by visual inspection (Fig 3). The ESE reader was able to detect signal at the test line down to 0.5 pg/mL. Four out of four blinded readers called 1 pg/mL positive, whereas three out of four blinded readers called 0.5 pg/mL positive. Results show that the AMD LFI has a limit of detection ≤ 1 pg/mL using this new magnetic immunoprecipitation protocol, which is an estimated 200-fold improvement over the 200 pg/mL LOD when using the standard testing protocol of the AMD LFI.

Testing Human Melioidosis Patient Urine Samples

While the magnetic immunoprecipitation protocol was effective in improving the analytical sensitivity of the AMD LFI when CPS was spiked into control urine samples, the next logical step was to analyze clinical samples. Therefore, we moved to assess the utility of the protocol with human melioidosis patient urine samples. To ensure that our testing reflected what is currently available from InBios, Inc., the new and improved AMD Plus LFI was used to evaluate the human urine samples.

Menzies School of Health and Research Testing. The Menzies School of Health and Research is located in northern Australia, a region where *B. pseudomallei* is endemic and has been defined as one of the highest risk zones [15]. We received a panel of small volume melioidosis patient samples from Menzies School of Health and Research and these samples were archived for future testing. Six samples from this panel were selected to validate the 1 mL magnetic immunoprecipitation protocol. These samples were all blood culture positive and had adequate volume for testing. The selected samples were analyzed via antigen-capture ELISA for the presence of CPS. Of the six samples, three had CPS present at a concentration that was within the detectable range of the ELISA, from 22 to 570 pg/mL (Table 1). The samples were then run on the AMD Plus LFI using the standard testing protocol to set a baseline sample reading. The results were visually evaluated as well as read with the Qiagen ESE Quant Reader. Two samples, 430-34 and 434-11, were positive with the standard testing protocol and had an OD of 168 and 12, respectively (Table 1). When subjected to magnetic immunoprecipitation, the LFI reading increased for the two positive samples, 818 and 99 respectively (Table 1). Furthermore, magnetic immunoprecipitation prior to running the samples on the AMD™ Plus LFI

resulted in three additional positive samples, 432-11, 438-3, and 438-7 (Fig 4). Sample ID 432-11 had a quantifiable concentration of CPS on the ELISA, but it was below the LOD of the AMD Plus LFI using the standard testing protocol. Sample ID 438-3 and 438-7 were below the LOD of the ELISA.

Lao-Oxford-Mahosot Hospital-Wellcome Trust Research Unit Testing**.** The Lao-Oxford-Mahosot Hospital-Wellcome Trust Research Unit is located in Southeast Asia, another region where *B. pseudomallei* is endemic and been defined as another high-risk zone [15]. We received a panel of melioidosis patient samples from Lao-Oxford-Mahosot Hospital-Wellcome Trust Research Unit and these samples were archived for future testing. Five samples from this panel that had previously undergone CPS quantification via antigen-capture ELISA were selected in part due to elevated volumes, approximately 10 mLs [124], as well as being culture positive at various sites (Table 2). These samples were run on the AMD Plus LFI using both the standard testing protocol and magnetic immunoprecipitation. Sample ID 879 was not tested using the standard testing protocol as the entire sample was used to test magnetic immunoprecipitation. However, the unfiltered 879 sample was previously tested on the AMD Plus LFI in the biosafety level 3 laboratory using the standard protocol and had a negative result (data not shown); no ESE Quant OD was obtained from testing the unfiltered sample. Of the remaining four samples, only 904 was positive with the standard testing protocol and had an OD of 12 (Table 2). Following magnetic immunoprecipitation, this sample had an increase in signal strength on the test line to OD 571 (Table 2). Furthermore, one additional positive test, sample ID 838, was observed following magnetic immunoprecipitation (Fig 5).

2.5 Discussion

Melioidosis is a neglected tropical disease that represents a significant public health burden spanning across several continents. This neglected disease is responsible for an estimated 89,000 deaths per year, much higher than the reported number as a result of the evidence pointing to under-reporting and limited knowledge of the disease by those in areas where it is not established as endemic [15]. The causative agent of this disease, *B. pseudomallei*, is intrinsically antibiotic resistant [127]. Consequently, it is imperative that a diagnosis is made early in the course of infection so the most effective antibiotics can be administered. In order to reduce the morbidity and mortality associated with the disease, a rapid diagnostic tool, the Active Melioidosis *Detect*™ lateral flow immunoassay (AMD LFI) has been developed by InBios International, Inc. in collaboration with our laboratory. The global burden of melioidosis is more prominent in resource limited areas, making the AMD LFI and now the AMD Plus LFI a potentially helpful diagnostic tool for melioidosis as it is easily employable in these areas and has a relatively quick time-to-result.

Based on the results obtained from our laboratory, CPS in clinically relevant biological fluids of melioidosis patient samples can range from nanograms per milliliter to picograms per milliliter in blood or serum and micrograms per milliliter to picograms per milliliter in urine [124]. The AMD Plus LFI, which detects CPS, can produce a respectful analytical sensitivity, but it appears that many patient samples contain undetectable or low picogram levels of CPS. The inherent barrier in analytical sensitivity is the restriction of the sample volume that can be run on most LFIs including the AMD Plus LFI. By conjugating a *B. pseudomallei* CPS reactive monoclonal antibody, 4C4, to Invitrogen Dynabeads M-270 Epoxy, we were able to use a magnet to rapidly isolate CPS from samples with volumes

≥1 mL prior to running those samples on the AMD LFI series. The development of this magnetic immunoprecipitation protocol to treat the samples prior to being used on the AMD LFI and AMD Plus LFI has resulted in 200-fold lower and 80-fold lower analytical limit of detection, respectively, based on the estimated limited of detection.

The benefit of the magnetic immunoprecipitation is two-fold. First, it allows the CPS present in 1 to 10 mLs of sample to be analyzed on the LFI, overcoming the limitations of the LFI sample volume. This is highly beneficial as it allows for the detection of low concentrations of CPS in larger sample volumes that would potentially be outside the detectable range for the AMD Plus LFI. Second, by isolating CPS from the biological fluid prior to running the LFI, possible matrix effects can be avoided. These matrix effects can contribute to false positives and streaking of the gold on the nitrocellulose membrane contributing to a test that is difficult to distinguish as positive or negative.

The magnetic immunoprecipitation developed in this study appears to be compatible with urine when tested on two different cohorts of patient samples. Using urine as the matrix is beneficial as serum is a challenging matrix to work with and acquire in comparison to urine. Additionally, it appears that the concentration of CPS may be lower in serum compared to urine [124]. All samples had their CPS concentration quantified via antigen-capture ELISA. Some samples that were found to contain CPS in the quantifiable range of the antigen-capture ELISA resulted in a negative result when testing them on the AMD Plus LFI with the standard testing protocol. After employing the magnetic immunoprecipitation protocol prior to running these samples on the AMD Plus LFI, multiple samples that were previously observed as negative became positive. Moreover, these results are particularly

encouraging given that some of these positive samples by LFI had CPS concentrations that were undetectable via ELISA. All the samples that were initially positive without magnetic immunoprecipitation were positive with magnetic immunoprecipitation and had increased signal strength at the test line. This is an important advantage as increased signal strength of the test line may also provide certainty for clinicians who may not have confidence in a melioidosis diagnosis based on a faintly positive test.

The results observed in this study are promising as we have demonstrated the ability to detect CPS in urine samples that were previously undetectable for CPS. This should potentially result in increased clinical sensitivity of the AMD Plus LFI. Furthermore, the instrumentation required for this concentrating in most cases can be found in a clinical laboratory. Therefore, this should be able to be performed in a clinical laboratory making it a potential option for rapidly identifying a challenging diagnostic case. Should a clinician suspect melioidosis even after a negative LFI result, this protocol could be implemented. This approach would be much faster than culturing, potentially allowing for the deployment of effective antibiotics sooner. The results here support the need for the further development of this protocol, which is currently ongoing. Finally, use of this method may be applicable to other infectious diseases that are hampered by low concentrations of target antigens in patient samples.

2.6 Figures and Tables

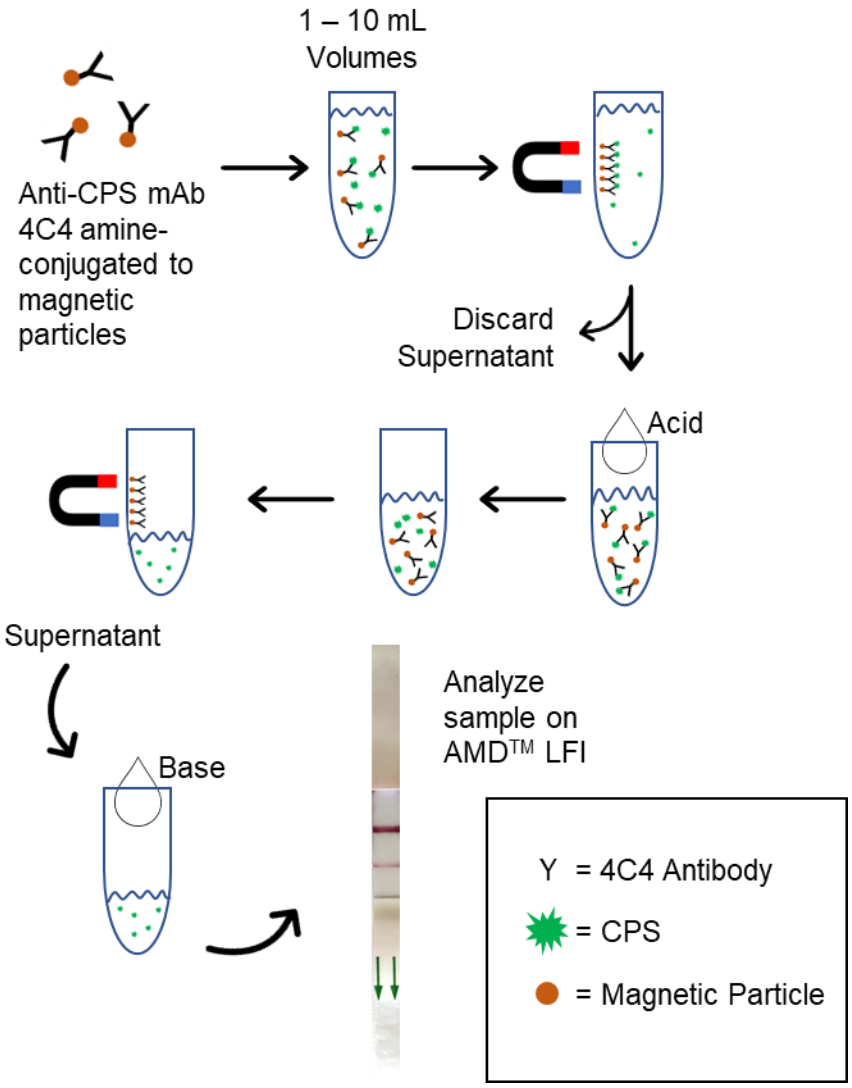

Figure 1. Schematic of magnetic immunoprecipitation testing protocol. Conjugate is added to a sample and incubated for 10 minutes while rotating. The sample is then placed on a magnet to allow for the removal of the supernatant. Acid is applied to the conjugate and then placed on a magnet to allow for the collection of the supernatant. The supernatant is neutralized with base and then analyzed by running it on the AMD LFI.

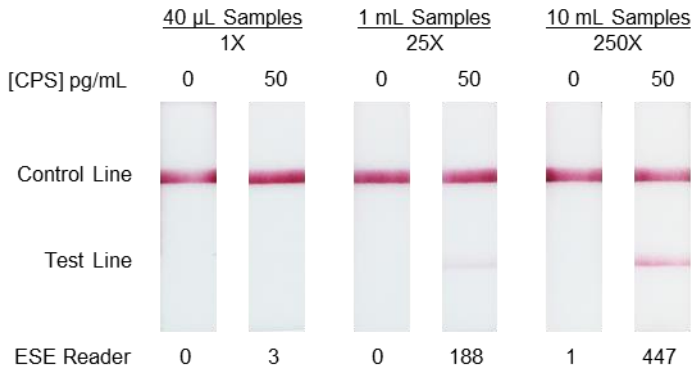

Figure 2. Testing of various sample volumes showed an increase in analytical sensitivity when using magnetic particles with larger volumes at the same concentration. Capsular polysaccharide at 50 pg/mL in PBS was tested using the testing protocol provided with the AMD™ LFI and compared to 1 mL and 10 mL samples at the same concentration of CPS using the magnetic immunoprecipitation protocol.

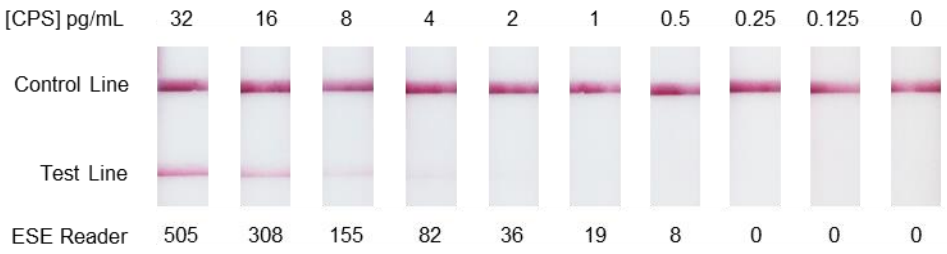

Figure 3. Capsular polysaccharide at various concentrations was spiked into 10 mL samples of pooled normal human urine and the limit of detection of CPS was determined to be ≤ 1 pg/mL. Samples magnetic immunoprecipitation and then run on the AMD™ LFI. LFIs were read after 15 minutes by the ESE Reader and four blinded readers to determine the limit of detection.

Figure 4. Images of AMD Plus LFI results from testing the human melioidosis samples obtained from Menzies School of Health Research. (A) Results from testing the samples using the standard testing protocol where sample ID 430-34 and 434-11 were positive. (B) Results from testing the samples using the magnetic immunoprecipitation protocol where sample ID 430-34, 432-11, 434-11, 438-3, and 438-7 were positive.

Figure 5. Images of AMD Plus LFI results from testing the human melioidosis samples obtained from Lao-Oxford-Mahosot Hospital-Wellcome Trust Research. (A) Results from testing the samples using the standard testing protocol where sample ID 904 was positive. (B) Results from testing the samples using the magnetic immunoprecipitation protocol where sample ID 838 and 904 were positive.

Table 1. CPS quantification and AMD Plus LFI results of 1 mL human melioidosis samples obtained from Menzies School of Health Research.

Sample ID	[CPS] pg/mL	Standard OD	MP OD
430-34	570	168	818
432-11	72	0	30
434-5	>LOD	0	0
434-11	22	12	99
438-3	>LOD	0	47
438-7	>LOD	0	18

Table 2. CPS quantification and AMD Plus LFI results of 10 mL human melioidosis samples obtained from Lao-Oxford-Mahosot Hospital-Wellcome Trust Research.

Sample ID	[CPS] pg/mL	Standard OD	MP OD
838[†]	>LOD	0	53
879[*‡§]	>LOD	NA	0
889*[†‡]	>LOD	0	0
900[‡§¶]	>LOD	0	0
903[‡]	>LOD	0	0
904*[§]	40	12	571

Culture positive site: [*]Blood, [†]Urine, [‡]Pus, [§]Throat Swab, [¶]Sputum.

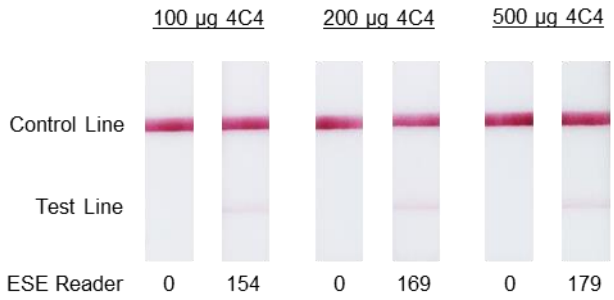

Supplementary Figure 1. Optimization of the amount of mAb 4C4 conjugated to Invitrogen Dynabeads M-270 Epoxy. Various amounts of anti-CPS mAb 4C4 conjugated to Invitrogen Dynabeads M-270 Epoxy and added to 1 mL PBS samples with CPS spiked in at 50 pg/mL. Following the magnetic immunoprecipitation protocol, the neutralized samples were run on the AMD™ LFI to evaluate optimal amount of mAb 4C4 for conjugation.

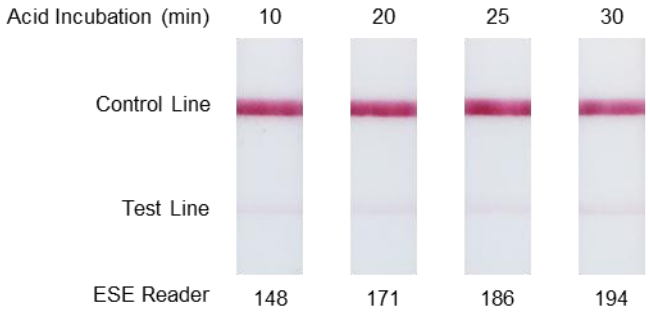

Supplementary Figure 2. Optimization of the length of the acid incubation for the magnetic particle protocol. During the magnetic immunoprecipitation protocol, the length of the acid incubation step was varied. Following completion of the protocol, the neutralized samples were run on the AMD^{TM} LFI to evaluate the optimal length for the acid incubation.

CHAPTER 3

Passive concentration of *Burkholderia pseudomallei* capsular polysaccharide from melioidosis urine samples for the enhanced detection on the Active Melioidosis Detect Lateral Flow Immunoassay

Heather R. Green[1], Derrick Hau[1], Peter Thorkildson[1], Viriya Hantrakun[2], Gumphol Wongsuvan[2], Direk Limmanthurotsakul[2], Bart J. Currie[3], Celeste Woerle[3], Mark Mayo[3], Christopher Myers[4], Caroline Balagot[4], Kathryn J. Pflughoeft[1], Marcellene A. Gates-Hollingsworth[1], David P. AuCoin[1]

Author Affiliates: [1] Department of Microbiology and Immunology, University of Nevada Reno School of Medicine Reno, Nevada, United States of America

[2]Mahidol-Oxford Tropical Medicine Research Unit, Mahidol University, Bangkok, Thailand

[3]Menzies School of Health Research, Charles Darwin University and Royal Darwin Hospital, Darwin, Australia

[4]Naval Health Research Center, San Diego, California, United States of America

Corresponding author: David AuCoin

Email: daucoin@med.unr.edu

3.1 Abstract

Burkholderia pseudomallei is a Gram-negative bacterium that is the causative agent of melioidosis, an infectious disease that is estimated to cause 89,000 deaths annually. The saprophytic bacterium is endemic to Southeast Asia and northern Australia. The disease manifestations can vary depending on the route of infection. Clinical manifestations can range from the nonspecific fever and myalgia to more severe symptoms such as pneumonia and sepsis. The gold standard for diagnosing melioidosis is culturing bacteria from a sample, which can take up to seven days to produce a result. Early diagnosis is essential for the favorable prognosis of the patient; therefore, a more rapid diagnostic testing method would be beneficial. The Active Melioidosis *Detect*™ Plus Lateral Flow Immunoassay (AMD Plus LFI) detects the capsular polysaccharide (CPS) of *B. pseudomallei*, which has been identified to be a reliable biomarker of a melioidosis infection. Here we examine the utility of passive CPS concentration of melioidosis urine samples, prior to analyzing the sample on the AMD Plus LFI, by comparison to unconcentrated or “neat” urine samples as well serum samples from the same patient. Our findings show this passive concentration method can produce positive tests from samples that are negative when testing the sample neat, as well as produce stronger test line intensities compared to testing neat samples. Our findings further support that urine is the optimal matrix for CPS detection in melioidosis patient samples based on testing paired urine and serum samples. Taken together, our findings support this alternative method for increasing clinical sensitivity and test line intensity thereby increasing the confidence of the clinician to establish a melioidosis diagnosis with the AMD Plus LFI.

3.2 Background

Burkholderia pseudomallei is a Gram-negative bacterium that is the causative agent of melioidosis, a deadly infectious disease. The estimated global burden of melioidosis is 165,000 cases and 89,000 deaths per year [15]. It's high mortality rate and lack of therapeutic options coupled with its potential to deliberately be misused as a bioterrorism agent resulted in *B. pseudomallei* being categorized as a Tier 1 Select Agent by the United States Department of Health and Human [7]. This bacterium is also an opportunistic pathogen putting those with diabetes, renal and lung disease, and even excessive alcohol use at a higher risk for developing a severe infection [128-130]. Up to 80% of patients who are diagnosed with melioidosis have one or more risk factors [131]. However, infections of healthy individuals have also been observed [132]. *B. pseudomallei* is often referred to as "the great mimicker" as the clinical presentation of infections are typically non-specific making symptom-based diagnosis difficult [110, 133]. These symptoms can range from generalized flu-like symptoms to pneumonia, organ failure, and sepsis [134]. Symptomology is often directly correlated to the route of infection, which can be through cutaneous inoculation, inhalation, or ingestion of the bacterium [37, 110]. These manifestations can range from generalized flu-like symptoms and can progress to pneumonia, organ failure, and sepsis if left untreated [130, 134].

B. pseudomallei is a soil-dwelling saprophyte that has been established to be endemic to Southeast Asia and northern Australia, however, the predicted global distribution of the bacterium reaches multiple countries in the tropics due to environmental suitability [15, 25]. The lack of surveillance and knowledge of the bacteria is one of the contributing factors for under diagnosis in areas outside of the established endemic regions. In

addition, the bacteria can be imported into countries outside the endemic region through sales of commercial goods, as demonstrated in the recent multistate outbreak of melioidosis in the United States in 2021 [18]. Four cases of melioidosis were diagnosed in people across four states and genome sequencing found these cases to all be related. These patients had no connections to each other and had not travelled to any country where *B. pseudomallei* is endemic. After extensive testing of samples from patients as well as soil, water, and consumer products in each home, the CDC identified an aroma spray that was manufactured in India was contaminated with *B. pseudomallei*. Even though these cases were in the United States, the case fatality rate (CFR) of this outbreak was 50% which is in line with the approximate CFR observed worldwide [6, 110, 135].

The current gold standard for diagnosing melioidosis is culture, which has 100% specificity, but only 60% sensitivity due to a low bioburden of the bacteria in clinical samples [39, 49]. Culturing can also take up to seven days to get a result due to a low bioburden during the course of an infection, which is detrimental to melioidosis patients, especially those that develop sepsis [136]. As *B. pseudomallei* is intrinsically resistant to many frontline antibiotics, a delay in diagnosis impedes the patient from receiving lifesaving therapies [135, 137]. While there are other diagnostic methods available, they are often costly and require highly trained lab personnel and lab equipment that is not readily available in regions where the bacterium is endemic [39, 138-140]. Lateral flow immunoassays (LFIs) are membrane-based assays that are ideal for diagnosing melioidosis because of their low-cost, ease of use, and lack of need for cold storage make them easily deployable in regions where melioidosis has the highest global burden. A typical LFI works by detecting a biomarker on a paper-based assay where the presence

of the biomarker indicates a positive result for a disease or other condition. This is accomplished using antibodies and colloidal gold nanoparticles for visualization without the need of specialized laboratory equipment.

The Active Melioidosis *Detect*™ Plus Lateral Flow Immunoassay (AMD Plus LFI) is a rapid, point-of-care (POC) diagnostic tool that has a 15-minute assay time [141]. The AMD Plus LFI is a second generation melioidosis assay from InBios, Inc. that detects the capsular polysaccharide (CPS) of *B. pseudomallei*, a biomarker of a melioidosis infection [43, 142]. This is done by using a CPS-reactive monoclonal antibody that is conjugated to colloidal gold nanoparticles to provide a colorimetric output to visualize the detection of CPS. CPS is a virulence factor that is a component of the outer membrane of the bacterium, which prevents phagocytosis and promotes dissemination and colonization [143, 144]. The structure of *B. pseudomallei* CPS consists of an unbranched homopolymer of 1,3-linked 2-*O*-acetyl-6-deoxy-β-D-*manno*-heptopyranose [145]. This high molecular weight antigen is typically shed by the bacterium during an infection and has been shown to be rapidly cleared via excretion through the urinary system *in vivo* [126]. The molecule appears to be greater than 300 kDa as visualized on a Western blot, which suggests it is too large to be filtered through the kidneys and excreted in urine [126, 142]. However, the molecule has been predicted to assume a rod-like shape with an estimated diameter of only 1.2 nm which is much smaller than the glomerular pore of 10 nm [126]. Previous research suggests that capillary flow could orient a molecule of this shape to align with the glomerular orifice facilitating filtration [126, 146]. Quantification of CPS in serum and urine from melioidosis patients has shown that CPS is present at higher concentration in urine, however, the concentration of CPS in patient samples has been found to vary greatly

[124]. Urine is a preferred clinical matrix compared to serum as it is an easily accessible sample, especially in countries with limited resources, and large volumes can be obtained with minimal effort. As such, this work was performed to further evaluate the diagnostic potential of urine for the diagnosis of melioidosis.

The AMD Plus LFI has several advantages as well as a few disadvantages. This rapid, POC diagnostic tool has a great analytical specificity and sensitivity, however, studies testing the AMD Plus LFI with melioidosis patient samples have observed low clinical sensitivity [55, 141]. One study performed in Laos found that the clinical sensitivity to vary by sample: 16.7% for serum, 25% for plasma, 66.7% for urine, 80% for sputum, and 85.7% for pus [141]. This is due to low concentrations of CPS in patient samples that are below the limit of CPS detection of the AMD Plus LFI [124]. To address this, methods to pre-concentrate CPS in urine samples is being evaluated. The goal of this study was to examine the utility of Vivapore BJP-5/30 concentrators to passively concentrate the CPS in urine samples from confirmed melioidosis patients across multiple cohorts prior to testing the sample on the AMD Plus LFI. We determined that this method of concentration was successful in producing positive AMD Plus LFI tests from samples that tested negative without concentration. Additionally, samples that tested positive neat had stronger test line intensities following concentration, which would provide clinicians with higher confidence in diagnosing a melioidosis infection through this diagnostic tool. One potential issue with this method is the concentration times, which varied between 2 and 24 hours. This is less time than the average time to diagnose through culture, though more rapid concentration time would be beneficial to make this a POC diagnostic. Implementation of a standard protocol for the concentration of CPS in a sample prior to

assessment on the AMD Plus LFI could contribute to a faster diagnosis of melioidosis patients in resource limited areas, which would potentially improve patient outcomes.

3.3 Methods

Sample Collection

Naval Health Research Center

Thirty fresh or archived remnant human urine samples were collected in the United States and were confirmed for *Escherichia coli* or *Klebsiella pneumoniae* by culture. Samples were collected between June 2021 and August 2021.

Menzies Health Center

Twenty-one urine samples were used in this study at Menzies Health Center (Darwin, Australia; Menzies). These samples were collected from patients from the Royal Darwin Hospital as part of the Darwin Prospective Melioidosis Study between December 2017 and December 2019. Eighteen samples were collected from confirmed melioidosis patients, two samples from patients reporting a fever, and one sample from a healthy endemic donor. The samples were archived at -80ºC for periods ranging between 0-716 days, with the exception of the sample from the healthy donor which was not frozen. For the melioidosis patients, diagnosis was confirmed via culturing of urine, blood, sputum, pus, and/or throat swab, and symptoms included genitourinary, pneumonia, and abscesses, and the culture matrix was chosen based on the symptoms.

Sunpasitthiprasong Hospital

Seventeen samples from confirmed melioidosis patients were obtained from Sunpasitthiprasong Hospital (Ubon Ratchathani Province, Thailand) and sent to Mahidol

Oxford Tropical Medicine Research Unit (MORU, Bangkok, Thailand) for testing. These samples were specifically chosen to represent urine culture negative samples. An additional panel of thirty paired urine and serum melioidosis patient samples, including urine culture positive samples, were obtained from MORU to be sent to the University of Nevada, Reno, where they were received into the biosafety level 3 for testing. These samples were obtained through active enrollment of patients with a melioidosis diagnosis confirmed via culturing or indirect fluorescent antibody test. The duration between hospital admission and enrollment into this study varied, with a maximum duration of fifty days.

Active Melioidosis *Detect*™ Plus Lateral Flow Immunoassay Testing

For Lateral Flow Immunoassay testing of serum, 30 µL of neat serum sample was applied to the sample pad of the AMD Plus LFI followed by two drops of Chase Buffer A (provided with the AMD Plus LFI kit). For LFI testing of unconcentrated urine, 50 µL of neat urine sample was applied to the sample pad followed by two drops of Chase Buffer A. For LFI testing of concentrated urine, approximately 50 µL of concentrated urine was applied to the sample pad of the AMD Plus LFI. For the testing conducted at the University of Nevada, Reno, the AMD Plus LFIs were run and imaged inside the biosafety level 3 biosafety cabinet once the AMD Plus LFI had run for 15 minutes and then visually evaluated as negative or positive, including faint test lines.

Urine Concentration

Depending on the sample, 0.5 mL to 5 mL was loaded into Vivapore BJP-5/30 concentrators (Pro-Chem, Massachusetts, USA) and left to passively concentrate.

Samples were first prefiltered using syringes with 0.45 μM Sartorius Ministart Filters (Sartorius, Goettingen, Germany), except for the samples tested at Menzies research Center which were not subjected to pre-filtration. Sample concentration varied from 24 minutes to 24 hours at room temperature to achieve an estimated 20-100-fold concentration. Following concentration 3-4 drops of 20X Lysis Buffer was added to the concentrated urine and allowed an additional five minutes to concentrate, with the exception of the samples tested at the University of Nevada, Reno which were not subjected to Lysis Buffer treatment.

3.4 Results

Specificity of Active Melioidosis *Detect*™ Plus with Vivapore BJP-5/30 concentration

To determine the specificity of the AMD Plus LFI using concentrated urine, potential cross-reactivity with other common urinary tract infection causing bacteria was assessed. As *Escherichia coli* and *Klebsiella pneumoniae* are common pathogens that cause urinary tract infections, samples from patients confirmed with either bacterium were selected for specificity testing [147-149]. For this assessment, thirty urine samples confirmed for *E. coli* or *K. pneumoniae* by culture were tested at the Naval Health Research Center (NHRC) before and after concentration, via Vivapore BJP-5/30 concentrators, on the AMD Plus LFI (Table 1). All thirty samples were negative when tested on the AMD Plus LFI prior to concentrating (Table 2). Each sample was then concentrated 50-100-fold was achieved and tested on the AMD LFI. Following this concentration method, all samples again tested negative (Table 1). The time required to concentrate each sample 50-100-fold varied, however overall, the average time to achieve the desired reduction in volume was longer for samples confirmed for *K. pneumoniae* compared to *E. coli*; mean of 102 minutes compared to 69 minutes respectively. No false positives were observed. Furthermore, urine sample storage did not affect the performance of the AMD Plus LFI when testing the sample neat or concentrated.

Testing of Menzies Cohort Melioidosis Patient Samples

AMD Plus LFI testing of urine from melioidosis patients as well as urine that was negative for *B. pseudomallei* from an endemic region was conducted at the Menzies Health Center

(Darwin, Australia). As with *E. coli* and *K. pneumoniae* samples, urine samples were first tested neat and then the sample was concentrated and tested. For this sample cohort, 21 samples were collected and tested. This cohort consisted of thirteen males and seven females ranging in age from 13-82 years. Eighteen samples were from confirmed melioidosis patients, which were confirmed via culture of one or more matrices including urine, blood, pus, sputum, and/or throat swab (Table 2). Culture matrix was varied because it is selected based on patient symptoms. The remaining three samples consisted of urine from two febrile, non-melioid patients and one healthy control. While the urine of the febrile patients was cultured, no samples were cultured for the healthy endemic donor. Each sample came from a unique donor, except samples 849-1 and 2 which were collected from the same patient before and after starting antibiotic treatment. In total, 12/17 patients were on *B. pseudomallei* specific antibiotic treatment, and the regimen duration varied from less than ten days for eight patients to 62-182 days for the remaining four patients. Of the twenty-one samples that were tested neat, only 3/18 (16.7%) of melioidosis samples tested positive on the AMD Plus LFI (Table 2). These three positive samples came from two patients that were urine culture positive and one blood culture positive patient. The three non-melioidosis samples tested negative. Following concentration, seven additional samples tested positive along with the three that tested positive neat, totaling 10/18 (55.5%) positive tests, including the five samples from urine culture positive patients resulting in 100% sensitivity for urine culture positive patients (Table 2). AMD Plus LFI positivity patients that were blood culture positive was 5/8 (62.5%) following concentration. Samples that were pus or throat swab culture confirmed all tested negative on the LFI both before and after concentration. Of note, samples 849-1 and 2 tested negative neat and 849-1 tested negative after concentration, however sample 849-2 tested positive after concentration. Interestingly, 849-1 was taken prior to antibiotic

treatment and 849-2 was taken four days after starting antibiotic treatment. Positivity may be a result of bacterial clearance and CPS excretion in the urine following antibiotic treatment. The three non-melioidosis samples tested negative following concentration, thus no false positives were observed. Excluding pus and throat swab culture confirmed patients, AMD Plus positivity was only 3/13 (23%) when testing the urine samples neat. However, upon urine concentration positivity improved to 10/13 (77%).

Testing of Sunpasitthiprasong Hospital Cohort at Mahidol Oxford Tropical Medicine Research Unit

As Southeast Asia is another area where *B. pseudomallei* is endemic, a cohort of samples from this area was acquired for testing. Patients from the Sunpasitthiprasong Hospital (Ubon Ratchathani Province, Thailand) were enrolled into a study and tested at the Mahidol Oxford Tropical Medicine Research Unit (Bangkok, Thailand). This cohort consisted of 17 samples from six females and eleven males with ages ranging between 28 and 74 years. This cohort was specifically selected to represent urine culture negative patients and does not accurately represent the melioidosis confirmed population. All patients had been confirmed to be infected with *B. pseudomallei* through culture of samples, except one patient, MRDT-125, who was confirmed via indirect fluorescent antibody test (Table 3). Urine sample collection was conducted up to fifty days post hospital admission with the average time between hospital admission and sample collection at 7.6 days. Patients were on *B. pseudomallei* specific antibiotics with the average duration being 5.3 days, except for two patients who were not on any antibiotics (MRDT-048 and 125). When testing urine samples from this cohort neat on the AMD Plus LFI, 7/17 (41.2%) were positive (Table 3). Four samples were collected from patients that

were blood culture positive and three were respiratory sample culture positive. For the ten samples that required concentration, sample volume ranged from 4.4-5 mL and time to concentrate ranged from 8-18 minutes to achieve a fold concentration between 50-100-fold. Following concentration, two more samples came back positive. One positive was from a blood culture positive patient giving overall positivity of 5/10 (50%) for the blood culture positive patients, which is a similar positivity to what was observed with blood culture positive patients on the MORU cohort. The other positive gained following concentration was collected from a respiratory sample positive patient giving overall positivity of 4/7 (57%) for respiratory positive patients (Table 3). In total, 9/17 positive tests were observed relating to 53% positivity from this cohort of urine culture negative melioidosis patients.

Testing of Sunpasitthiprasong Hospital Cohort at the University of Nevada, Reno

Additional patients from Sunpasitthiprasong hospital were recruited to be part of a cohort whose samples were sent to the University of Nevada, Reno to be tested. Unlike previous testing, this testing consisted of paired serum and urine to be evaluated as a direct comparison of both matrices. All patients had been confirmed to be infected with *B. pseudomallei* through culture or indirect fluorescent antibody test of various sample sites at the time of admission to Sunpasitthiprasong hospital (Table 4). This cohort consisted of six females and twenty-four males with ages ranging between 21 and 74 years. Sample collection was conducted during enrollment, which occurred up to sixteen days post hospital admission. The average time between hospital admission and sample collection was 4.8 days, meaning that most patients were on *B. pseudomallei* specific antibiotics at the time of sample collection, with an average treatment time of 7.6 days. All paired blood

and urine samples from each patient were taken within fifteen minutes from each other. Following sample collection, each sample was tested again for the presence of *B. pseudomallei,* and the culture results are shown in Table 4.

AMD Plus LFI Testing of Urine

All thirty urine samples were tested neat on the AMD Plus LFI. Of the 30 samples that were tested, 12/30 (40%) were positive, 3/30 (10%) samples were scored as weakly positive due to a very faint line, and 15/30 (50%) samples were negative (Table 4). Of the twelve samples that tested positive, five were urine and blood culture positive, one was urine culture only positive, and the remaining six were culture negative. Of the three samples that tested weakly positive, MRDT-095 was urine, blood, and other site culture positive, MRDT-084 was blood and other site culture positive, and MRDT-087 was culture negative. The positivity of this cohort for testing neat samples was the highest observed in this multi-site study.

Samples that tested negative or weakly positive were concentrated 10-100-fold over 4-24 hours. There was no obvious visual indicator between samples that would require a longer concentration time, except for MRDT-054. This sample appeared to contain a substantial amount of red blood cells which potentially impaired the ability of the concentrator to function properly, resulting in only a 25-fold concentration (SFig 1). Following concentration, 7/15 (47%) of samples tested positive (Table 4). Figure 1A shows an example of a sample (MRDT-070) that tested negative pre-concentration and positive post-concentration. Of the three samples that tested faintly positive pre-concentration,

only 2/3 (67%) of samples (MRDT-084 and 087) tested positive with a stronger test line intensity following concentration (Fig 1B). It was unexpected that one of these samples tested negative as concentration of the sample should result in a higher concentration of CPS and therefore all samples were expected to result in a positive with a stronger test line intensity than when testing neat. One sample which tested negative following concentration, MRDT-095, was unexpected as this patient was confirmed *B. pseudomallei* positive through culturing of urine, blood, and throat at the time of sample collection. Potential explanation of the reversal in the test includes the removal of cell associated CPS during the pre-filtration step of the sample prior to concentration or that the unconcentrated test result was incorrectly evaluated as a positive. The AMD Plus was scored as a faint positive when testing the sample neat and it is possible that there was a misinterpretation of the positivity of the LFI when being visually evaluated (Fig 1C).

In terms of total positivity from testing urine samples in this cohort, 21/30 (70%) samples were positive. Not including the potential false positive of MRDT-095, 7/9 (78%) of samples from urine culture positive patients had a positive test. Of the four samples that were blood culture positive (with or without another site being culture positive), 2/4 (50%) tests were positive. 2/3 (67%) of samples from patients that were only culture confirmed from a site other than urine or blood were positive. For the remaining fourteen samples that were from melioidosis confirmed patients but were culture negative at the time of sample collection, 10/14 (71%) were positive via LFI.

AMD Plus LFI Testing of Serum

Extensive clinical testing was performed on the samples collected from each patient. At the time of sample collection, thirteen patients were negative for *B. pseudomallei* through culture of blood, urine, throat, and sputum, and seventeen patients were *B. pseudomallei* positive through culture of one or more of the aforementioned sample types (Table 4). All thirty serum samples were tested on the AMD Plus LFI. Of the thirty samples that were tested, only 3/30 (10%) of samples were read as positive and an additional two samples (6.67%) were weakly positive (Table 4). Of the positive samples, MRDT-040 was positive for *B. pseudomallei* via IFA of a respiratory sample and MRDT-133 was positive for *B. pseudomallei* via blood culture prior to enrollment into this study. Interestingly, samples MRDT-040 and 133 tested negative for *B. pseudomallei* through culturing but were positive on the AMD Plus LFI. Of the samples that tested negative, nine were confirmed to be blood culture positive at the time of sample collection. Of note, four serum samples did not flow properly on the LFI, and a successful re-test of these samples were conducted. Additionally, when testing serum samples, it was observed that the nitrocellulose of these LFIs did not resolve well, resulting in a membrane that was not easy to read visually (SFig 2). Furthermore, all samples that tested positive in serum also tested positive in urine. All samples that tested positive in serum also tested positive with neat urine and the serum LFI had a fainter test line, apart from MRDT-109 which maxed out the LFI visual evaluation in both matrices. These results further support that urine is the optimal matrix for CPS detection in melioidosis patients.

3.5 Discussion

Melioidosis, caused by *B. pseudomallei*, is a multifaceted infectious disease that is a threat to public health. The bacterium is endemic in many countries around the world, has a high mortality rate, and has the potential to be used as a bioterrorism agent. Enhanced surveillance of the bacteria in endemic areas has resulted in decreased mortality rates, but it is suspected that many countries have a greater burden than what is reported [15]. Given that melioidosis presents with a range of nonspecific symptoms, rapid diagnosis is crucial. *B. pseudomallei* is intrinsically resistant to many frontline antibiotics, therefore early administration of the appropriate antibiotics is imperative for treatment of the infection and overall patient outcome. Even with the appropriate antibiotics, the CFR can be as high as 40% [135]. The current gold standard for diagnosis is culturing, but it's extended time to diagnosis and relatively low sensitivity of 60% are major shortcomings for this diagnostic method [39]. This can be contributed to the low bioburden of the bacteria, taking days to get a result via culturing. The AMD Plus is a rapid test that can performed at the point-of-care. As a diagnostic tool, LFIs are easy to use and are ideal for low technology settings as they do not require any specialized laboratory equipment. The AMD Plus LFI works by detecting CPS, which forms a capsule around the bacterium and is an important virulence factor [150]. *In vivo* studies have shown that the majority of CPS appears to be shed and is rapidly filtered through the kidney and accumulated in the urine [126]. Here and in previous studies comparing serum and urine for CPS detection in patient samples, the analysis of urine consistently results in a higher positivity rate [124]. Thus, urine should be considered the preferred matrix for CPS detection on the AMD Plus LFI.

Enrichment of CPS in patient samples using Vivapore BJP-5/30 concentrators was evaluated with the goal of enhancing the detection of CPS on the AMD Plus LFI as a means to overcome sample with concentrations of CPS outside the detection limit. To ensure that the AMD Plus LFI was specific to a *B. pseudomallei* infection, a preliminary specificity study was conducted. Since urine is an important matrix for detecting CPS on the AMD Plus LFI, it is pertinent to test for potential cross-reactivity with other bacteria that may be found in urine during an infection. Furthermore, it is important to test urine collected from infected patients via this concentration method and determine if false positive reactions could occur from this process. *E. coli* and *K. pneumoniae* are two bacteria that commonly cause urinary tract infections [147-149]. Thirty urine samples testing positive for *E. coli* or *K. pneumoniae* via culture were selected for analysis to validate the specificity of this new protocol implementing the Vivapore BJP 5/30 concentrators. All thirty samples tested negative on the AMD Plus LFI, both pre- and post-concentration.

To assess the sensitivity of the assay following passive concentration, samples were collected and tested at multiple sites with the goal of evaluating the utility of concentrating urine samples. The testing conducted at Menzies included urine samples from eighteen confirmed melioidosis patients, two febrile patients that did not have melioidosis, and one healthy donor. Of the eighteen melioidosis urine samples, three tested positive pre-concentration and an additional seven tests were positive on the AMD Plus LFI post-concentration. This cohort included patients that were urine culture positive, blood culture positive, or were positive from culturing of another matrix. Five the urine samples were collected from patients who were confirmed to be urine culture positive and all five of these

samples tested positive on the AMD Plus LFI either with or without concentration. Urine from blood culture positive patients showed increased AMD Plus positivity following concentration, with only 1/8 samples positive pre-concentration and 5/8 positive post-concentration. Overall, in this cohort urine concentration improved the sample positivity rate for samples collected from blood culture positive patients. Results indicate a higher positivity rate when testing patients that are urine culture positive, though positive AMD Plus LFIs were observed with patients who were urine culture negative.

Urine was collected from four patients that were only confirmed melioidosis positive via culture of their pus. Interestingly, none of the urine samples from these patients were positive on the AMD Plus LFI, with or without concentration, indicating that urine concentration might not be suitable for patients with abscesses. However, the AMD Plus LFI can be used with several matrices and patients presenting with skin abscesses can have pus and/or abscess fluid samples collected for testing. The AMD LFI has been shown to have higher sensitivity with pus and abscess fluid samples when compared to blood samples based on studies in Laos and India [55, 141, 151, 152].

Of note from the Menzies cohort are samples 849-1 and 849-2 which were taken from the same patient before and after starting antibiotic treatment, respectively. Sample 849-1 was negative both pre- and post-concentration and 849-2 was negative pre-concentration but was positive post-concentration. AMD Plus positivity may reflect bacterial clearance and CPS excretion in the urine as a result of the antibiotic treatment. Although this was only seen in one patient in this cohort, further studies should be performed to test multiple patients throughout antibiotic treatment. Finally, the three known non-melioidosis samples

that were collected from patients in an endemic region tested negative with this concentration method.

Among urine samples collected from urine culture negative patients that were tested at MORU, seven were positive on the AMD Plus LFI pre-concentration and two were positive post-concentration. Confirmation of melioidosis for these patients were either from blood culture or culture of another site, and it is important to note that this is not an accurate representation of melioidosis population as any urine culture positive patients were excluded. From this cohort, the overall positivity rate of urine testing was 4/10 for blood culture positive patients and 3/7 for throat/sputum culture positive patients before concentration, post-concentration 5/10 and 4/7 were pos, respectively. *B. pseudomallei* negative urine samples were not available for testing and therefore specificity of concentrated urine from this endemic region was not assessed. However, the AMD Plus LFI positivity rate of the urine samples distinguished based on the sample site that was culture positive was similar to what was observed at the other testing sites.

The samples that were collected at Sunpasitthiprasong hospital and shipped to the University of Nevada, Reno included not only urine, but also serum. These paired serum samples were collected from the patient within fifteen minutes of the urine collection. This enabled us to test both matrices and get a direct comparison of AMD Plus LFI positivity of serum and urine for each patient. We found that urine had a higher positivity rate compared to serum, which is similar to what has been observed in a separate study [124].For serum testing, only 5/30 samples tested positive on the AMD Plus LFI. Comparatively, when testing pre-concentrated urine, 15/30 tested positive. Every positive

sample in serum was also positive in urine, often at a much stronger test line intensity making a definitive positive easier to read. From this study and others, serum does not need to be tested on this diagnostic platform. Following concentration of the eighteen urine samples that tested negative (15) or weakly positive (3), 9/18 tested positive on the AMD Plus LFI. Overall positivity for urine, irrespective of concentration, was 21/30, which is an improvement over the positivity seen with serum testing. The eight samples that remained negative had various culture results. Three were culture positive at the time of sample collection, via either blood, urine, and/or another site. The five remaining negative samples were culture negative at the time of sample collection, which could potentially be contributed to the low sensitivity of culturing. Interestingly, of these five that were culture negative at the time of sample collection, three were initially confirmed *B. pseudomallei* positive via culturing of a pus sample. Pus from these patients was not collected and therefore not tested on the AMD Plus LFI. Similar to what was observed with the testing performed at other sites in this study, patients with abscesses suspected of having melioidosis were negative on the AMD Plus LFI with this testing method. This might be a result of shed CPS not being cleared in the urine at high concentrations in patients with localized infections. These patients might need to have their pus tested as the relevant matrix for AMD Plus LFI [55, 141, 151, 152].

In conclusion, this large study consisted of testing melioidosis patient samples from two regions where *B. pseudomallei* is endemic. In total, samples from sixty-five melioidosis patients were tested on the AMD Plus LFI. These melioidosis patients were confirmed via culturing or IFA of samples from one or more sites. Across the entire study, positivity for the AMD Plus was 25/65 when testing urine pre-concentrated and 40/65 following

concentration. While this is not as sensitive as culture, it should still be viewed as an alternative diagnostic as it is more rapid for time to result and is inexpensive. The AMD Plus LFI can be used in tandem with culturing to rapidly detect the bacteria in the culture bottle after 12 hours of growth, which can speed up diagnosis substantially [151]. Concentration of urine samples with the Vivapore BJP-5/30 concentrators resulted in a 23% improvement in sensitivity on the AMD Plus LFI. Our findings further support that urine is the preferred sample matrix for CPS detection on the AMD Plus LFI. Given that melioidosis is most common in regions around the world that might not have the resources to support extensive culturing of multiple samples from a patient, testing of unconcentrated and concentrated urine on the AMD Plus LFI in the method evaluated here is a logical first step for the rapid diagnosis of melioidosis at the point-of-care in areas that have limited resources.

3.6 Figures and Tables

Table 1. Summary of the *E. coli* and *K. pneumoniae* confirmed patient samples and results of urine samples tested on the AMD Plus LFI at the Naval Health Research Center, before and after concentrating.

Sample ID	Culture confirmed organism	AMD Plus Results	
		Pre-Concentration	Post-Concentration
INBP001	*E. coli*	Negative	Negative
INBP002	*E. coli*	Negative	Negative
INBP003	*E. coli*	Negative	Negative
INBP004	*E. coli*	Negative	Negative
INBP005	*E. coli*	Negative	Negative
INBP006	*E. coli*	Negative	Negative
INBP007	*E. coli*	Negative	Negative
INBP008	*E. coli*	Negative	Negative
INBP009	*E. coli*	Negative	Negative
INBP010	*E. coli*	Negative	Negative
INBP011	*E. coli*	Negative	Negative
INBP012	*E. coli*	Negative	Negative
INBP013	*E. coli*	Negative	Negative
INBP014	*E. coli*	Negative	Negative
INBP016	*E. coli*	Negative	Negative
INBP018	*E. coli*	Negative	Negative
INBP021	*E. coli*	Negative	Negative
INBP022	*E. coli*	Negative	Negative
INBP023	*E. coli*	Negative	Negative
INBP024	*E. coli*	Negative	Negative
INBP027	*E. coli*	Negative	Negative
INBP028	*E. coli*	Negative	Negative
INBP029	*E. coli*	Negative	Negative
INBP030	*E. coli*	Negative	Negative
INBP026	*K. pneumoniae*	Negative	Negative
INBP015	*K. pneumoniae*	Negative	Negative
INBP017	*K. pneumoniae*	Negative	Negative
INBP020	*K. pneumoniae*	Negative	Negative

INBP025	*K. pneumoniae*	Negative	Negative
INBP019	*K. pneumoniae*	Negative	Negative

Table 2. Summary of the patient samples and results of urine samples tested on the AMD Plus LFI at the Menzies Health Center, before and after concentrating.

Sample ID	*Bp* confirmed in	AMD Plus Results	
		Pre-Concentration	**Post-Concentration**
999-19	Urine and blood	Positive	Positive
411-1	Urine and sputum	Negative	Positive
550-14	Urine and blood	Negative	Positive
900-4	Urine	Negative	Positive
412-17	Urine	Positive	Positive
1100-2	Blood and Sputum	Negative	Negative
568-16	Blood and Pus	Negative	Positive
614-1	Blood and Pus	Negative	Negative
659-15	Blood	Positive	Positive
753-1	Blood	Negative	Positive
849-1	Blood	Negative	Negative
849-2	Blood	Negative	Positive
956-18	Blood	Negative	Positive
928-1	Pus	Negative	Negative
401-15	Pus	Negative	Negative
567-3	Pus	Negative	Negative
1101-2	Pus	Negative	Negative
570-1	Throat swab	Negative	Negative
211-11	None	Negative	Negative
574-7	None	Negative	Negative
1189-1	None	Negative	Negative

Table 3. Summary of the patient samples and results of urine samples tested on the AMD Plus LFI at the Mahidol Oxford Tropical Medicine Research Unit, before and after concentrating.

Sample ID	*Bp* confirmed in			Urine AMD Plus	
	Urine culture	Blood culture	Other site culture*	Pre-Concentration	Post-Concentration
MRDT-020	Negative	Positive	Negative	Negative	Positive
MRDT-027	Negative	Positive	Negative	Positive	ND
MRDT-029	Negative	Positive	Negative	Negative	Negative
MRDT-041	Negative	Positive	Negative	Positive	ND
MRDT-042	Negative	Positive	Negative	Negative	Negative
MRDT-046	Negative	Positive	Negative	Negative	Negative
MRDT-055	Negative	Positive	Negative	Positive	ND
MRDT-068	Negative	Positive	Positive	Positive	ND
MRDT-105	Negative	Positive	Negative	Negative	Negative
MRDT-125**	Negative	Negative	Negative	Negative	Negative
MRDT-007	Negative	Negative	Positive	Positive	ND
MRDT-014	Negative	Negative	Positive	Negative	Negative
MRDT-022	Negative	Negative	Positive	Positive	ND
MRDT-048	Negative	Negative	Positive	Negative	Positive
MRDT-056	Negative	Negative	Positive	Negative	Negative
MRDT-111	Negative	Negative	Positive	Negative	Negative
MRDT-126	Negative	Negative	Positive	Positive	ND

*Culture of sputum or throat swab

**Positive via indirect fluorescent antibody test

Table 4. Summary of the patient samples and results of paired serum and urine samples tested on the AMD Plus LFI at the University of Nevada, Reno.

Sample ID	*Bp* confirmed in			Serum AMD Plus	Urine AMD Plus	
	Urine	Blood	Other*		Pre-Concentration	Post-Concentration **
MRDT-035	Positive	Positive	Positive	Negative	Positive	ND
MRDT-036	Positive	Positive	Positive	Negative	Negative	Positive
MRDT-038	Positive	Negative	NA	Negative	Positive	ND
MRDT-063	Positive	Positive	Positive	Positive	Positive	ND
MRDT-074* **	Positive	Positive	NA	Negative	Negative	Negative
MRDT-095	Positive	Positive	Positive	Negative	Positive	Negative
MRDT-096	Positive	Positive	Positive	Negative	Positive	ND
MRDT-107	Positive	Positive	Positive	Positive	Positive	ND
MRDT-109	Positive	Positive	Positive	Positive	Positive	ND
MRDT-081	Negative	Positive	Positive	Negative	Negative	Positive
MRDT-082	Negative	Positive	Positive	Negative	Negative	Negative
MRDT-084	Negative	Positive	Positive	Negative	Positive	Positive
MRDT-132	Negative	Positive	NA	Negative	Negative	Negative
MRDT-054	Negative	Negative	Positive	Negative	Negative	Negative

MRDT-058	Negative	Negative	Positive	Negative	Negative	Positive
MRDT-070	Negative	Negative	Positive	Negative	Negative	Positive
MRDT-040	Negative	Negative	NA	Positive	Positive	ND
MRDT-099	Negative	Negative	NA	Negative	Positive	ND
MRDT-117	Negative	Negative	NA	Negative	Negative	Negative
MRDT-123	Negative	Negative	NA	Negative	Negative	Positive
MRDT-133	Negative	Negative	NA	Positive	Positive	ND
MRDT-018	Negative	Negative	Negative	Negative	Positive	ND
MRDT-045	Negative	Negative	Negative	Negative	Negative	Positive
MRDT-060	Negative	Negative	Negative	Negative	Positive	ND
MRDT-087	Negative	Negative	Negative	Negative	Positive	Positive
MRDT-098	Negative	Negative	Negative	Negative	Negative	Positive
MRDT-104	Negative	Negative	Negative	Negative	Negative	Negative
MRDT-110	Negative	Negative	Negative	Negative	Negative	Negative
MRDT-119	Negative	Negative	Negative	Negative	Positive	ND
MRDT-128	Negative	Negative	Negative	Negative	Negative	Negative

*NA refers to samples that only had their urine and blood cultured.

**ND refers to samples that were not concentrated as they were AMD Plus reactive using pre-concentrated urine.

***Initial confirmation of diagnosis via indirect fluorescent antibody test.

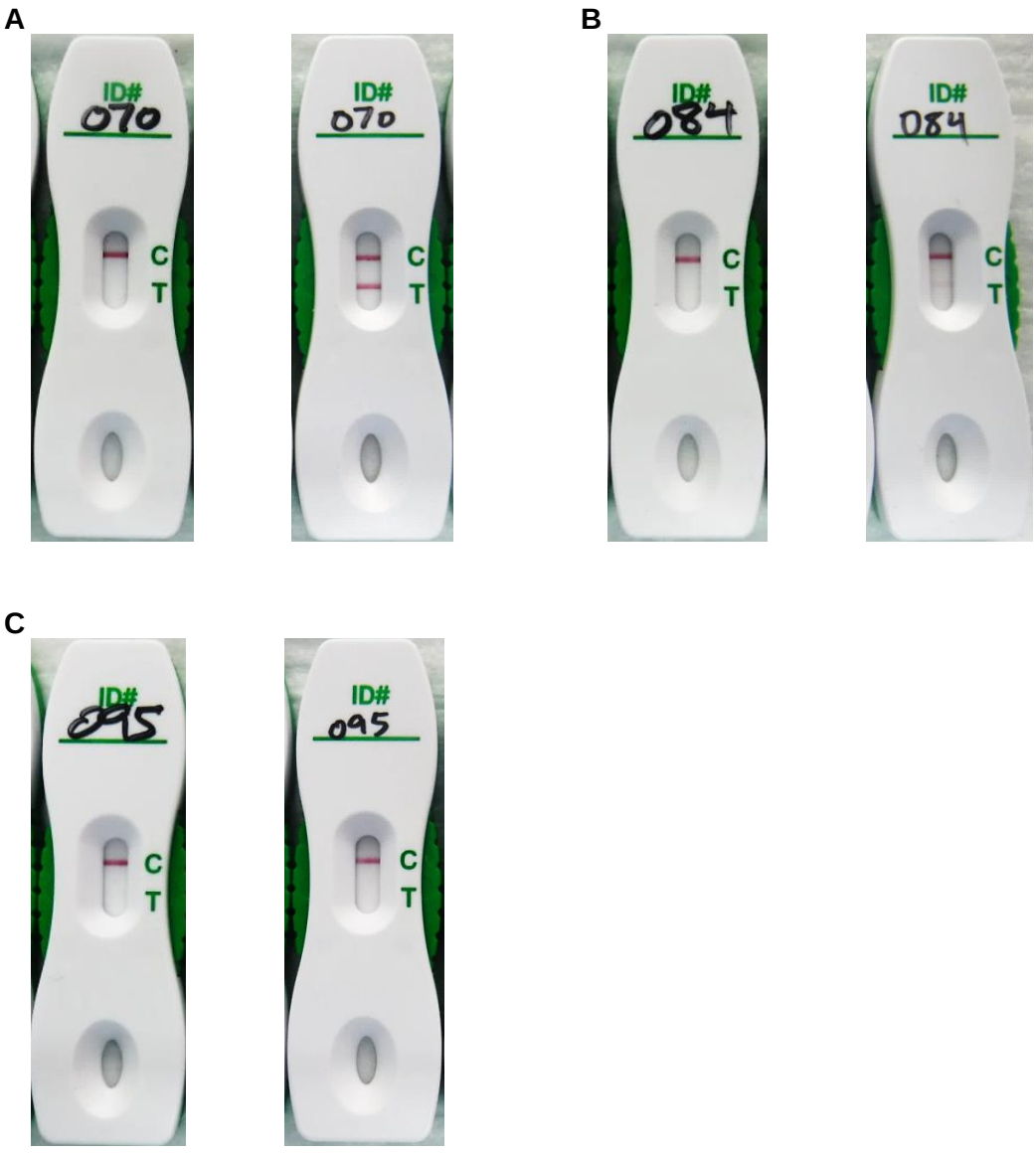

Figure 1. Images of AMD Plus lateral flow immunoassays showing results when testing samples pre- and post-concentration. (A) Sample MRDT-070 was evaluated as negative pre-concentration (left) and positive post-concentration (right). (B) Sample MRDT-095 was evaluated by two operators as faintly positive pre-concentration (left) and negative post-concentration (right).

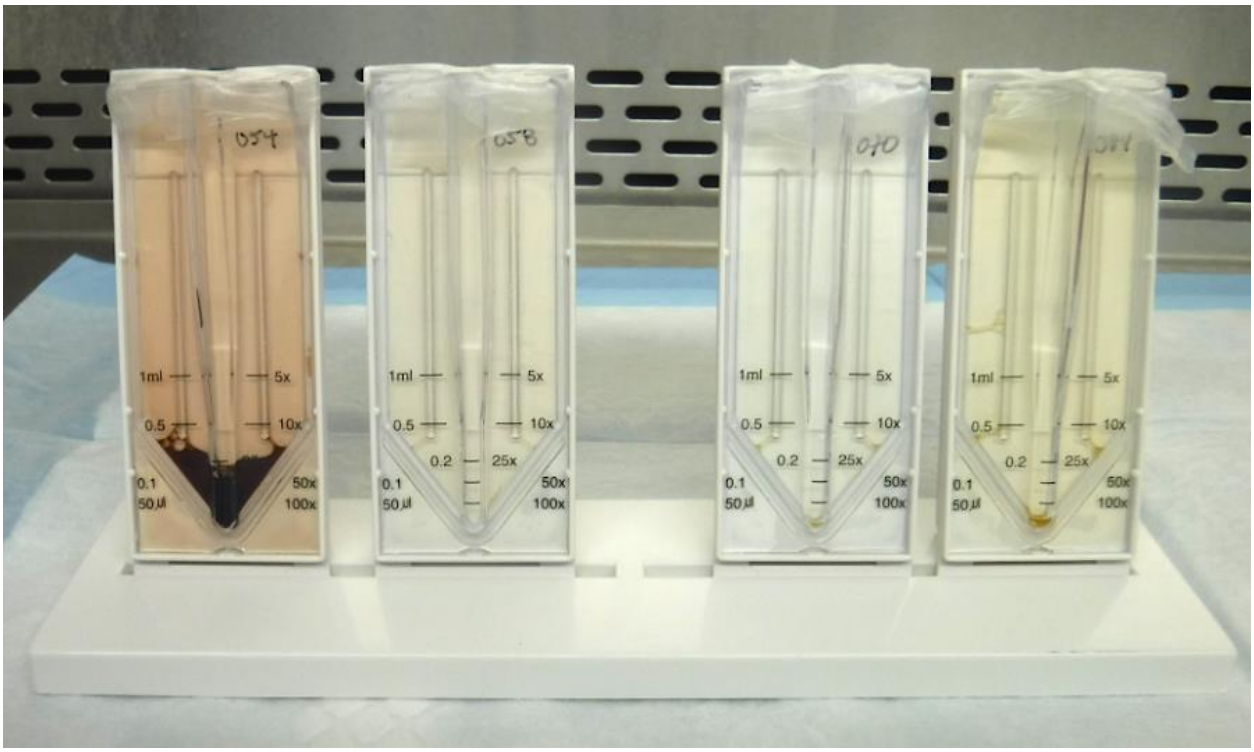

Supplemental Figure 1. Image of Vivapore BJP-5/30 concentrators used for concentrating urine samples from melioidosis patients. Sample MRDT-054 did not fully concentrate and appears to contain a substantial amount of red blood cells.

Supplemental Figure 2. Image of serum samples tested on AMD Plus after 15 minutes of run time. Samples MRDT-082 and 087 did not fully resolve, impairing the ability to visually evaluate the test. Sample MRDT-084 did not run and had to be retested.

CHAPTER 4

Development of a point-of-care immunoassay for Ebola virus disease through the detection of Ebolavirus soluble glycoprotein

Heather R. Green[1], Derrick Hau[1], Sujata G. Pandit[1], Jose Arias-Umnana[1], Chelsea C. Chung[1], Haley L. DeMers[1], Lesly Carrasco[1], Abigail F. Foster[1], Anjana Dissanayaka[1], Marcellene A. Gates-Hollingsworth[1], David P. AuCoin[1]

Author Affiliates: [1] Department of Microbiology and Immunology, University of Nevada Reno School of Medicine Reno, Nevada, United States of America,

Corresponding author: David AuCoin

Email: daucoin@med.unr.edu

4.1 Abstract

Ebola virus disease (EVD) is a deadly infectious disease that is caused by an infection with Ebola virus (EBOV). The case fatality rate (CFR) for EVD can be as high as 90%, making it one of the deadliest viral diseases. Transmission of the virus can occur through the direct contact of mucus membranes with an infected animal or human. Early detection is imperative to prevent the spread of disease and reduce the risk of a potential epidemic by isolating known infected patients. The current gold standard for diagnosing EVD is polymerase chain reaction, assays which requires complex laboratory equipment and highly trained personnel, a technique that is not easily accessible in resource-limited areas. There is a great need for an EBOV rapid diagnostic test that can be implemented at the point-of-care (POC). Multiple lateral flow immunoassays (LFIs) have been developed for this need and have received emergency use authorization. Many of these tests rely on the detection of Ebola virus VP40 antigen, however, soluble glycoprotein (sGP) has the potential to be a better biomarker for EVD rapid detection as it can be detected early in the course of an infection. The goal of this study was to produce an EBOV sGP LFI prototype. A library of seventeen monoclonal antibodies reactive to EBOV sGP were produced and characterized via enzyme-linked immunosorbent assay, surface plasmon resonance, and Western immunoblotting. From this mAb library, LFI prototypes were developed and assessed for the potential use as a rapid POC diagnostic for EVD.

4.2 Background

Ebolaviruses are highly pathogenic filoviruses that are the causative agent of an acute hemorrhagic fever called Ebola virus disease (EVD), which has a case fatality rate (CFR) of up to 90% [153, 154]. The genus *Ebolavirus* is comprised of six species: *Zaire ebolavirus* (ZEBOV)*, Sudan ebolavirus* (SUDV)*, Bundibugyo ebolavirus* (BDBV), *Taï Forest ebolavirus* (TAFV), *Reston ebolavirus* (RESTV), and *Bombali ebolavirus* (BOMV) [155]. The most concerning species is ZEBOV, which accounts for the majority of outbreaks, followed by SUDV and BDBV, respectively. The most severe outbreak to date was the 2013-2016 West African outbreak in which ZEBOV resulted in over 11,000 deaths [156]. New outbreaks are still occurring and in 2021 there were two outbreaks of ZEBOV with a CFR just over 50%. The virus is endemic in sub-Saharan Africa and the natural host of the virus has yet to be elucidated. African fruit bats have long been suspected, even more so with the newest species BOMBV being identified in bats [155]. In addition to spreading through direct contact with infected fruit bats and nonhuman primates (NHP), the virus can also be transmitted through direct contact with an infected patient or infected bodily fluids, including blood, saliva, tears, urine, semen, and sweat [72, 157]. As such, there is a great need to identify EVD patients early, prior to the onset of severe symptoms, and isolate them to prevent further spread of the disease.

The incubation period of EVD in humans is 2-21 days and clinical presentation initially appear to be nonspecific, making diagnosis based on symptoms challenging for early infections [74]. The current gold standard for diagnosing EVD is polymerase chain reaction (PCR), an assay that requires laboratory infrastructure and highly trained laboratory personnel that is not easily accessible in the areas most affected in recent outbreaks [158].

During the recent West African outbreak, samples had to be transported to centralized laboratory facilities, which had an average delay of five days from sample collection to result [159]. A simulation found that decreasing the delay from 5 days to 1 day in 60% of EVD cases would drop the viral attack rate, the chance of an at-risk population contracting the disease, from 80% to almost 0% [160]. This EBOV epidemic highlighted the need for a point-of-care (POC), rapid diagnostic that can detect EVD early in the course of an infection. The lateral flow immunoassay (LFI) is a membrane based rapid diagnostic test (RDT) that uses antibody-based technology to detect a biomarker of a disease. This diagnostic platform can be employed at the POC without the need for specialized laboratory equipment or highly trained personnel. LFIs are affordable, do not require refrigeration, and can deliver a result in less than twenty minutes, making them an excellent diagnostic tool for EVD. In fact, an LFI called ReEBOV which detects the EBOV protein VP40 has been given emergency use authorization (EUA) by the FDA. However, the EUA has since been revoked as it was not sensitive enough to diagnose early EVD infections [161]. A more clinically sensitive RDT is needed to ensure patient isolation can be performed early to mitigate the spread of disease.

Most RDTs, including ReEBOV (Corgenix, Inc.) and OraQuick Ebola (OraSure Technologies), detect VP40 as it is the most abundant viral protein and is present in the blood of patients with high viremia [162, 163]. However, VP40 does not appear to be a good target for early detection of EVD when viral load is low, an observation noted across multiple field trials of the RDTs [164, 165]. A previous study in our lab found that a GP-specific LFI prototype was more sensitive at detecting an early EBOV infection in nonhuman primates when compared to a viral matrix protein VP40-specific LFI prototype

and the ReEBOV Antigen Rapid Test [166]. The *GP* gene is one of only seven genes that make up the EBOV genome and it encodes for three proteins: GP, soluble GP (sGP), and small sGP (ssGP) [167]. During transcription of *GP*, the viral polymerase encounters a site of seven adenosine residues (7A), and it is at this 7A site where transcriptional editing occurs. About 70% of the products are a result of an unedited seven uridine (7U) transcript, which produces sGP [168, 169]. Of the remaining products, 25% are the result of the viral polymerase stuttering and resulting in either an 8U edited transcript, GP, or a 9U edited transcript, ssGP. sGP is expressed at a higher level than GP and is also known to be secreted in high quantities from infected cells [170, 171]. Given that sGP is produced during the early stages of the disease, an LFI that can detect sGP needs to be investigated for its ability to diagnose early EVD [172].

The goal of this study was to isolate high affinity monoclonal antibodies (mAbs) that are reactive to sGP for the development of a point-of-care lateral flow immunoassay. Seventeen mAbs reactive to sGP were isolated from mice immunized with either sGP or EBOV virus like particles (VLPs), noninfectious particles that contain VP40 and GP to mimic the morphology of the live virus. Unpurified mAbs were initially assessed via Western immunoblot against gamma-irradiated viral cell lysate from five species of *Ebolavirus*: EBOV, SUDV, TAFV, BDBV, and RESTV, as well as in the LFI format in both capture and detection positions. The combined data was used to identify the top performing mAbs, which were then further characterized through enzyme-linked immunosorbent assay (ELISA), surface plasmon resonance (SPR), and Western immunoblotting. Initial prototype LFIs were optimized and validated to be reactive to

recombinant sGP. Finally, gamma-irradiated ZEBOV infected Vero E6 cell lysate was assessed to ensure this early prototype was capable of detecting native sGP.

4.3 Methods

mAb Production

Female CD1 mice, 6-8 weeks old (Charles River Laboratories, Inc., Wilmington, MA, USA), were immunized with recombinant EBOV sGP (IBT Bioservices, Rockville, MD) mixed with Freund's adjuvant (MilliporeSigma, Billerica, MA) via intraperitoneal injection. The initial immunization was performed using Freund's complete adjuvant with subsequent boosts using Freund's incomplete at weeks 4 and 8. A final boost of recombinant protein without adjuvant was administered intravenously three days prior to splenectomy. Sera samples were collected via retro-orbital survival bleeds to determine serum antibody titers via sGP indirect ELISA (described below). Hybridomas were produced using the ClonaCell™-HY Hybridoma Kit (STEMCELL Technologies, Vancouver, Canada) with selection in a liquid medium. Archived splenocytes from CD1 mice that were immunized with nano-eVLPs were also used to create hybridomas [166]. Fusions were performed with these archived splenocytes using P3x63Ag.651 fusion partner and hybridoma cells were produced using standard techniques [173].

sGP Indirect ELISA

96-well microtiter plates were coated recombinant EBOV sGP (IBT Bioservices) in phosphate buffered saline (PBS) overnight at room temperature. Plates were washed with PBS containing 0.05% Tween-20 (PBS-T) and blocked for 90 minutes at 37°C with PBS containing 5% non-fat milk and 0.1% Tween 20 (blocking buffer). Primary antibodies (mouse sera or purified mAbs) were diluted in blocking buffer and two-fold serial diluted across the plate. Primary antibodies were incubated for 90 minutes at room temperature

and then washed with blocking buffer. Next, plates were incubated for 60 minutes with horseradish peroxidase (HRP) labeled goat anti-mouse IgG antibody (SouthernBiotech, Birmingham, AL) or IgG subclass specific goat anti-mouse antibody (SouthernBiotech). Plates were then washed with PBS-T and incubated for 30 minutes at room temperature with tetramethylbenzidine (TMB) substrate (Kirkegaard & Perry Laboratories, Inc., Gaithersburg, MD). 1M phosphoric acid (H_3PO_4) was used to stop the reaction. Plates were read to obtain colorimetric data at an optical density of 450nm (OD_{450}).

Western Immunoblot

Standard semidry Western blot procedure was performed using 1 µg recombinant EBOV sGP (IBT Bioservices) or 10 µL of gamma-irradiated *Zaire ebolavirus* antigen preparation (NR-31807) (BEI Resources, Manassas, VA, USA). Samples were mixed with 6x loading buffer, either non-reducing or reducing, and diluted in a total volume of 200 µL. For denaturing conditions, samples were boiled for 10 minutes. Samples were separated on 10% SDS gel (Bio-Rad Laboratories, Hercules, CA, USA) and transferred to nitrocellulose membrane (Bio-Rad). A Miniblotter system (Interchim, Montluçon, France) was used to enable the use of multiple antibodies to probe one antigen preparation. Primary mAbs were used at 200 ng/mL or 1µg/mL to probe the membranes and secondary HRP-labeled goat anti-mouse IgG (SouthernBiotech) was used at a 1:10,000 dilution for detection. Signal was detected with SuperSignal™ West Femto Maximum Sensitivity Substrate (Thermo Fisher Scientific, Waltham, MA, USA) and images were taken using a ChemiDoc XRS system (Bio-Rad).

Lateral Flow Immunoassay (LFI) Screening

Initial screening for LFI pairs was performed with each mAb in either the capture or detection position of the LFI. Testing was conducted using a default LFI prototype to evaluate reactivity to recombinant sGP in PBS and non-specific binding in chase buffer. Briefly, 5 µL of gold conjugate at OD 10 was added to 40 µL of chase buffer with or without sGP spiked in at a concentration of 100 ng/mL in a microtiter well. The LFI was then immersed into the well and allowed for the entire sample to flow onto the nitrocellulose membrane through capillary action. The LFI was then immersed into another well containing 100 µL of chase buffer and the LFI was allowed to fully resolve, approximately 20 minutes. LFIs were then visually evaluated and read using an ESE-Quant lateral flow reader (Qiagen, Hilden, Germany). The LFIs were assessed based on the signal intensity at the test line when running 100 ng/mL recombinant sGP minus nonspecific signal when running chase buffer only as determined by the ESE reader (Supplemental Table 1). The best performing pairs were selected for further optimization.

Antigen-Capture ELISA

96-well microtiter plates were coated with 100 µL/well of mAb 2HG13 (2.5 µg/mL) in PBS overnight. Plates were washed using PBS-T and blocked for 90 minutes at 37 °C with 300 µL/well of blocking buffer. Recombinant EBOV sGP (IBT Bioservices) was added to the first well at a concentration of 250 ng/mL and two-fold serial diluted down the plate in blocking buffer, as above, for a final volume of 100 µL/well. Following an incubation of 90 minutes at room temperature, plates were washed with blocking buffer and then incubated for 60 minutes with HRP-labeled 2HG12 at 5 ug/mL in blocking buffer at room temperature. Plates were washed with PBS-T and incubated for 30 minutes with 100 µL/well of TMB

substrate. The reaction was stopped with 100 µL/well of 1M phosphoric acid (H_3PO_4) and then read at an optical density of 450 nm (OD_{450}).

Surface Plasmon Resonance (SPR)

Surface plasmon resonance was performed using a Biacore X100 instrument (GE Healthcare, Piscataway, NJ). A His Capture Kit (Cytiva) was used to immobilize an anti-His antibody on the surface of a CM5 chip. To analyze the binding kinetics and affinity of mAbs to recombinant EBOV sGP (IBT Bioservices), 12.5 ng/mL of His-tagged recombinant protein was captured and binding was then measured by injecting mAbs at five concentrations (50 µg/mL or 200 µg/mL with two-fold serial dilutions) in triplicate. Kinetic analysis was performed using a 1:1 model on the Biacore X100 Evaluation Software (Cytiva).

sGP LFI Prototype

The sGP LFI prototype was developed using mAbs 2HG12 (capture) and 2HG5 (detection). CN140 (Sartorius, Gottingen, Germany) nitrocellulose membranes were striped with unlabeled antibodies using the BioDot XYZ platform (BioDot, Irvine, CA). Capture mAb was striped at 1 mg/mL to serve as the test line. Goat anti-mouse Ig (SouthernBiotech) was striped at 1 mg/mL to serve as the control line. After the striping of antibodies, membranes were dried at 37˚C for 30 minutes. LFIs were assembled with the nitrocellulose membrane and an overlapping C083 cellulose fiber sample pad (MilliporeSigma), to serve as the wicking pad, on an adhesive backing card. LFIs were cut to 4 mm strips and stored in foil pouches with desiccants. 2HG5 was passively adsorbed

to 40 nm colloidal gold particles (DCN Diagnostics, Carlsbad, CA), blocked, and then concentrated to an optical density of 10 at 540 nm. This gold labeled antibody was used as the detection mAb for the LFI prototype.

4.4 Results

mAb Production and Reactivity

Seventeen hybridoma cell lines were established from female CD1 mice immunized with either recombinant sGP or nano-eVLP mixed with Freund's adjuvant. From these cell lines, cloning was performed to isolate single monoclonal cell lines that produced an antibody reactive to recombinant sGP via indirect ELISA. After establishing monoclonality, mAbs were purified and an indirect ELISA was performed to determine subclass for each mAb. This library is made up of IgG1, IgG2a, and IgG2b (Table 1). Western immunoblots were performed using recombinant sGP in both non-reduced (Fig. 1A) and reduced (Fig. 1B) conditions to validate reactivity. Reactivity varied, but each mAb was reactive to sGP in either or both conditions. MAb 2HG12 was the only mAb that was not reactive to sGP in the reduced form, although it was reactive in the non-reduced form, suggesting reactivity to a conformational epitope. Additionally, all mAbs from the sGP immunization were less reactive to the non-reduced form then the reduced form. mAbs were then evaluated for reactivity against ZEBOV antigen preparations produced from infected Vero E6 cells (gamma-irradiated) via Western immunoblotting. As was observed with sGP, reactivity to the gamma-irradiated virus varied in the non-reducing conditions (Fig. 1C) compared to the reducing conditions (Fig. 1D). All mAbs were reactive to at least one condition with many being reactive to both. Finally, Western immunoblotting was performed to identify binding of isolated mAbs to gamma-irradiated cell lysate containing Vero E6 cells that were infected with SUDV, BDBV, and TAFV to screen for pan-reactivity. Reactivity of these mAbs to the different species varied, though none were pan-reactive (data not shown). To note, 2HG5 was reactive to ZEBOV, SUDV, and BDBV.

LFI Screening

To identify mAb pairs for the development of an sGP LFI prototype, all mAbs were evaluated in the capture and detection position and tested for reactivity with recombinant sGP. This initial testing was conducted using a standard concentration of 100 ng/mL of sGP diluted into chase buffer and the test line signal intensity was compared to that of chase buffer alone as a negative control. The best pairs were evaluated as having the most signal in the presence of sGP and the least signal in the absence of sGP based on visual evaluation as well as being quantified using a Qiagen ESE-Quant lateral flow reader. This criterion was used to down select a possible 289 combinations, to the top thirteen performing pairs. Of note, many mAbs did not detect sGP in this pairwise assay even though they were shown to be reactive to sGP on an indirect ELISA. This could indicate that many of these mAbs contain epitopes that are spatially near one another on the protein thereby sterically hindering binding in these paired assays. Nonetheless, some pairs were able to detect sGP in this assay platform and were further evaluated by screening 100, 10, and 0 ng/mL, identifying the four best mAb pairs which included 2HG12 in the capture position and 2HG2, 2HG5, 2HG10, or 2HG13 in the detection position.

Antigen-Capture ELISA

Following screening in the LFI format, as well as some initial screening of unpurified mAbs against gamma-irradiated viral cell lysate via Western immunoblotting (data not shown), the top eight performing mAbs (1HG1, 1HG2, 1HG6, 2HG2, 2HG5, 2HG10, 2HG12, and 2HG13) were selected to be further characterized. MAbs were evaluated via antigen-capture ELISA to identify the best pair for detection of recombinant sGP. All eight mAbs were conjugated to HRP and each mAb was assessed in the capture and detection

position for an antigen-capture ELISA. As was observed in the initial LFI screening, many pairs did not detect sGP in this format, though two pairs performed well: 2HG12 in the capture position with 2HG2-HRP at the detection and 2HG13 in the capture position with 2HG12-HRP as the detection. These two pairs were further evaluated, and the best performing pair was determined to be 2HG13 as the capture mAb and 2HG12-HRP as the detection mAb. Following optimization of this assay, sGP serially diluted in buffer was run in triplicate to determine the limit of detection. These conditions gave an LOD of 95 pg/mL as calculated by 2x background. The standard curve for the average of these three runs is shown in Figure 2.

Surface Plasmon Resonance

Kinetic analysis via SPR was also performed on the top eight mAbs. Experiments were performed in triplicate and evaluated with the BIAevaluation software using a 1:1 binding analysis to determine the association rate (k_a), dissociation rate (k_d), and affinity (K_D; $K_D = k_d/k_a$) for each mAb (Table 2). All mAbs had similar association rates and affinity except for 1HG6, which at $5.5x10^3$ $M^{-1}s^{-1}$ had a 10-fold slower association rate compared to the other seven mAbs that were evaluated. Dissociation rates varied between the mAbs. 1HG6, 2HG2, 2HG10, and 2HG13 had similar dissociations rates, which were between $1.4\text{-}1.8x10^{-4}$ s^{-1}. The other four mAbs had relatively better dissociations rates that varied between $3.6x10^{-4}$ and $6.9x10^{-5}$ s^{-1}. 1HG1 had the highest affinity (lowest K_D), however it was not identified to be a good mAb pairing in either the LFI or the antigen-capture ELISA using this library, so it was excluded from further analysis. All mAbs except for 1HG6 have relatively high affinity as determined by SPR analysis, which supports their usefulness to be integrated into a rapid diagnostic for EVD.

LFI Prototype Development and Reactivity with Inactivated ZEBOV

After the initial screening of LFI prototypes, as well as characterization based on antigen-capture ELISA and SPR evaluation, the top performing mAb pairs were selected for further optimization in the LFI format. These two pairs contain 2HG12 as the capture antibody and either 2HG5 or 2HG13 as the colloidal gold labeled detection antibody. LFI prototype development included optimization of nitrocellulose membrane and chase buffer. Both pairs had reactivity with recombinant sGP spiked into chase buffer down to 10 ng/mL. 2HG5 as the detection had very low nonspecific binding, whereas 2HG13 nonspecific binding was more pronounced through visual evaluation (Figure 3). As the 2HG5 detection prototype produced a stronger test line in the presence of recombinant protein and less nonspecific binding, it was chosen as the top performing prototype following initial optimization.

Availability of gamma-irradiated cell-lysate from ZEBOV infected Vero E6 cells from BEI Resources enabled confirmation of binding of mAbs to the native conformation of the protein in the LFI format. Two dilutions of the cell lysate were tested, and a dose-response was observed (Figure 4). Uninfected Vero E6 cell lysates were tested as a negative control, and although some nonspecific binding was observed, the signal when testing the ZEBOV infected cell lysate was much higher indicating there is reactivity with this prototype to native protein.

4.5 Discussion

Lateral flow immunoassays are well established RDTs and there continues to be increased use of this technology for the rapid, point-of-care testing of infectious diseases. These inexpensive, easy to use and store tests can provide a diagnosis in under twenty minutes, making them an excellent diagnostic platform for a disease such as EVD. EBOV is endemic in sub-Saharan Africa where infrastructure and trained lab personnel are not easily accessible. The current gold standard diagnostic method for EVD is PCR, but as was observed in the West African epidemic, there can be a high time delay for diagnosis which can result in patients not being isolated and further the spread of the deadly virus. Easily deployable RDTs, such as lateral flow immunoassays, have the ability to change the course of an Ebola epidemic as was modeled by Dhillon *et al.* [160]. An RDT that can be performed at the POC has the potential to quickly identify infected patients allowing for the rapid isolation of infected individuals which can ultimately mitigate further spread of the virus. Here we produced a panel of monoclonal antibodies that are reactive to EBOV sGP, characterized the antibodies through multiple immunoassay platforms, and selected pairs of mAbs for the development of a prototype LFI.

Previous RDTs that have been developed for EVD have targeted VP40, a protein that is known to be the most abundant protein expressed from the EBOV genome. However, a previous study in our lab indicated that surface GP was a better target when compared directly to VP40 for detection of an early infection in non-human primates [166]. Knowing that GP is not the main product of *GP*, and that sGP is produced about three times more than GP indicated that sGP has the potential to be an even better biomarker for an EVD RDT [168]. The panel of mAbs isolated and characterized in this study are reactive to

recombinant sGP. Throughout the characterization process, it was evident that the reactivity of the mAbs varied within and across the assays that were conducted to characterize them. Initial characterization included testing the mAbs against the protein directly, however, with the end goal of developing an LFI prototype, it was important to test these antibodies on the LFI platform early in the study. The LFI uses a form of sandwich binding so it is imperative that antibody pairs that can bind to the antigen simultaneously be identified for the developmental process. Initial screening of all pairs on the LFI platform indicated that many mAbs that reacted very strongly with sGP in Western immunoblotting did not work well when paired with the other antibodies in this panel. Of the 289 combinations of pairs that were tested, only thirteen pairs showed reactivity to sGP on the LFI. Interestingly, this might be explained by the epitopes that are recognized by the mAbs. If the mAb's epitope on sGP is spatially in close proximity to one anotheror are identical, steric hinderance could be a factor. Epitope mapping of these highly reactive mAbs could provide insight into why some of these mAbs did not work well as pairs.

Following the initial LFI screening and Western blot analysis, the top performing mAbs were selected to undergo further characterization. It is important to note that for this study we are most interested in mAbs that function well as a pair. While some mAbs may appear to have stronger reactivity to recombinant protein, it was important for us to down select to pairs that had the potential to be implemented in the LFI. 2HG1 has good reactivity to sGP on the Western immunoblot, however when testing on the LFI platform with the other mAbs minimal reactivity was observed. As such it was not selected for further characterization. The 8 mAbs that were further characterized were first used to develop an antigen-capture ELISA. Screening and optimization resulted in 2HG13 being used as

the capture mAb and 2HG12-HRP as the detection mAb. As 2HG12 was identified to be a good capture mAb for the LFI, it was not surprising to see it also be included in the final pair for the ELISA. This again could be in part due to the epitopes of the other mAbs. The analytical limit of detection for this ELISA was determined to be 95 pg/mL, but it is not as accessible as an LFI for diagnosing EVD in low-technology settings. This ELISA is could still be very useful for understanding the biomarker availability during disease progression, such as to determine the concentration of sGP in patient samples.

SPR analysis of association and dissociation rates these top eight mAbs indicate that these mAbs have a high affinity for recombinant sGP. This is important as higher affinity mAbs have more potential in immunoassays, as evident from their analytical sensitivity which should correlate to clinical sensitivity. 2HG12 was identified as having the fastest association rate, which could indicate why it was a superior mAb in the assays developed in this study. However, it did have one of the lowest affinities relative to the other mAbs that were evaluated, which again shows the importance of antibodies' ability to work in tandem. This implies the potential of a more sensitive assays if another antibody besides 2HG12 could work as a pair with another antibody from this library. Overall, the mAbs used in the optimized assays all displayed affinities less than 10 nM.

Two pairs stood out as the best performers throughout the optimization process of the pairs that worked best from the initial screening of the mAbs in the LFI format. 2HG12 as the capture mAb and 2HG5 or 2HG13 as the detection mAb showed reactivity down to 10 ng/mL. Through optimization of these prototypes, 2HG5 as the detection mAb slightly outperformed 2HG13 as determined by the intensity of the test line. After selecting the top

pair for the LFI format it was important to continue testing with antigen preparations of EBOV as it is critical for this prototype to be reactive to native protein, not just recombinant protein which was used for all previous LFI optimization. Testing of this prototype with cell lysate from ZEBOV infected Vero E6 cells indicated reactivity with native protein. However, assessment of this prototype with Vero E6 cell lysate, both visually and with the ESE Quant LFI reader that measures the signal strength in mm*mV, showed the need for further optimization to reduce the nonspecific binding. This assay is an early prototype and further optimization can be conducted to overcome this nonspecific binding. As this LFI undergoes further development, many components could change including chase buffer, membranes, capture and/or detection mAbs.

There are six species of *Ebolaviruses*, four of which are known to cause infections in humans. Of these four species, ZEBOV is responsible for causing the most infections. The LFI prototype developed in this study was shown to be reactive to ZEBOV sGP, which is an important step in the development of a RDT for EVD. However, with three other species known to cause disease in humans, pursuing the development of a pan-reactive sGP LFI would also be of importance. mAbs from this study and potential future studies should be tested in pairs to determine if a pan-reactive LFI can be established. 2HG5 was reactive to the three species known for causing the most infections, and it was the mAb that was selected for the LFI prototype developed in this study. There is potential for 2HG5 to be developed into an LFI with a different capture mAb that also has reactivity for these species which would enable this LFI to be used in outbreaks caused by any of these species. Additional studies that need to be conducted include specificity testing of other pathogens that are common the in geographical region of Ebola that cause similar

symptoms and optimization in serum as the testing matrix. Our findings here support that the pairs in both the LFI and the antigen-capture ELISA are highly sensitive to EBOV sGP, but there is room for the identification and implementation of a capture mAb that is pan-reactive to allow for these assays to be implemented in all suspected Ebolavirus cases, regardless of the species. This study provided the groundwork for the development of an EBOV sGP LFI with the goal of early diagnosis of EVD and further optimization of this necessary to address the need of a POC diagnostic for EVD.

4.6 Figures and Tables

Table 1. Summary of subclass and immunization strategy for library of seventeen monoclonal antibodies reactive to recombinant EBOV sGP isolated in this study.

mAb	Subclass	Immunization
1HG1	IgG2b	sGP
1HG2	IgG2b	sGP
1HG4	IgG1	sGP
1HG6	IgG1	sGP
2HG1	IgG2b	Nano-eVLP
2HG2	IgG2b	Nano-eVLP
2HG3	IgG1	Nano-eVLP
2HG4	IgG2b	Nano-eVLP
2HG5	IgG2b	Nano-eVLP
2HG6	IgG1	Nano-eVLP
2HG7	IgG1	Nano-eVLP
2HG8	IgG1	Nano-eVLP
2HG9	IgG2a	Nano-eVLP
2HG10	IgG2a	Nano-eVLP
2HG11	IgG2b	Nano-eVLP
2HG12	IgG2b	Nano-eVLP
2HG13	IgG2b	Nano-eVLP

Table 2. Kinetics analysis and affinity determination of EBOV sGP mAbs by surface plasmon resonance.

mAb	k_a ($M^{-1}s^{-1}$)	k_d (s^{-1})	K_D (nM)
1HG1	1.43E+04	1.91E-05	1.30
1HG2	1.67E+04	6.69E-05	3.99
1HG6	5.49E+03	1.73E-04	31.6
2HG2	2.58E+04	1.27E-04	5.06
2HG5	3.11E+04	6.85E-05	2.21
2HG10	3.94E+04	1.39E-04	3.54
2HG12	4.12E+04	3.60E-04	8.65
2HG13	3.26E+04	1.57E-04	4.63

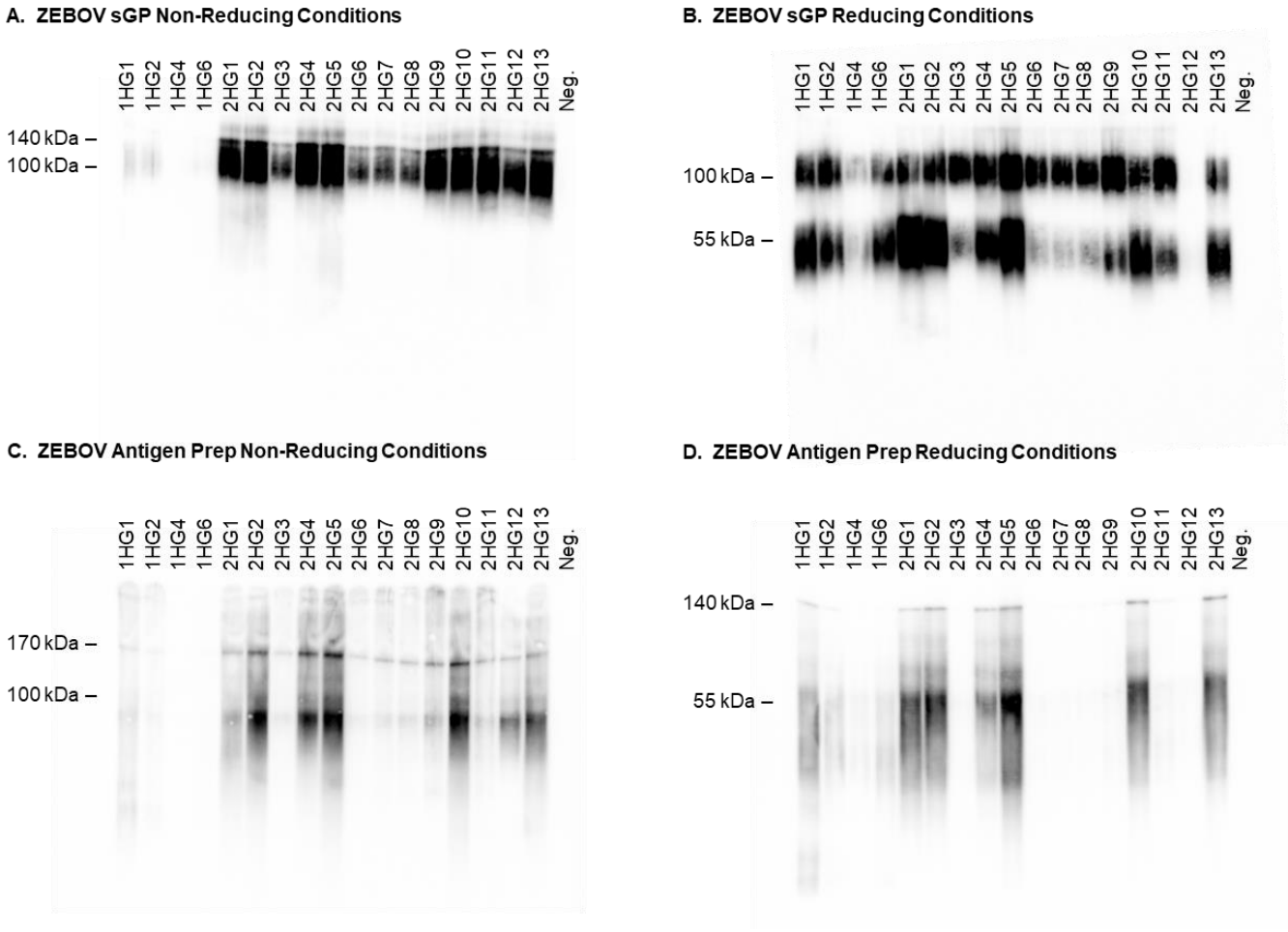

Figure 1. Reactivity of mAbs to recombinant sGP and gamma-irradiated ZEBOV antigen preparations via Western immunoblotting using a Miniblotter system. mAb reactivity was evaluated using 1 µg recombinant sGP in non-reducing conditions (Panel A) or reducing conditions (Panel B) and 10 µL of antigen preparation from infected Vero E6 cells in non-reducing conditions (Panel C) and reducing conditions (Panel D).

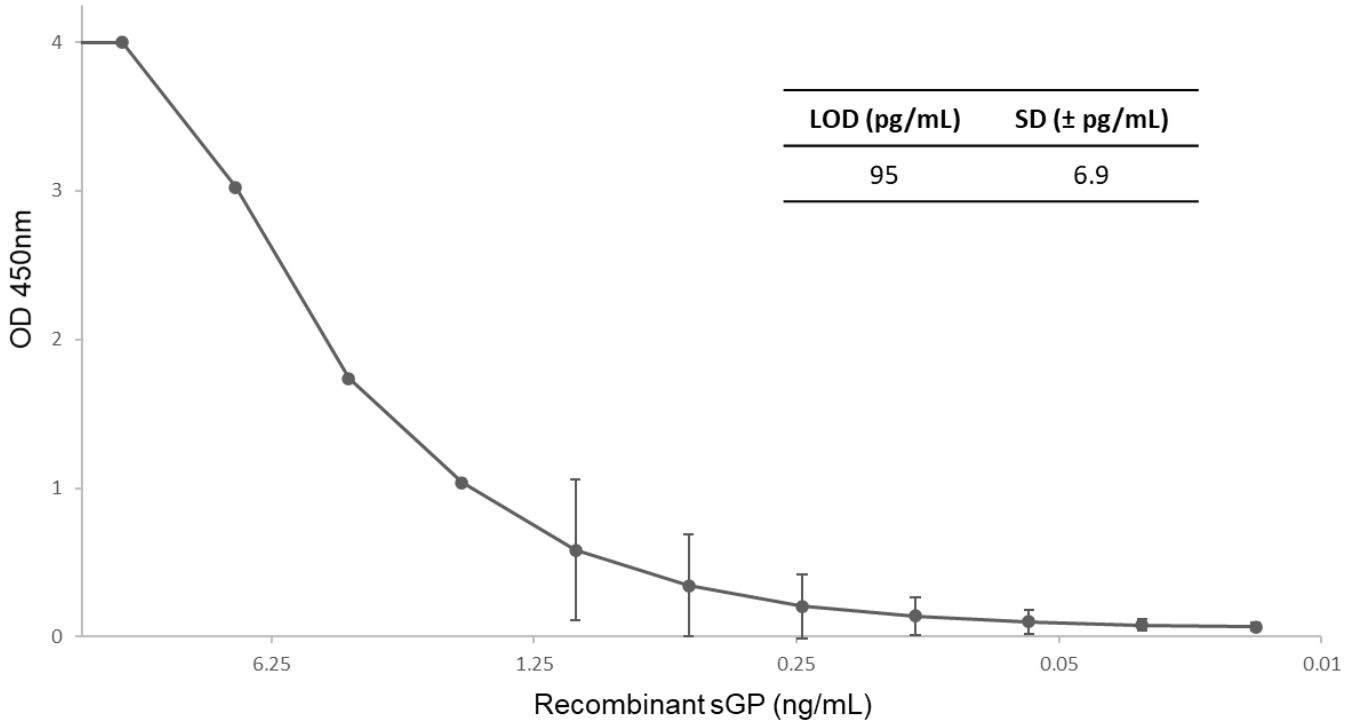

Figure 2. Optimized recombinant sGP antigen-capture ELISA limit of detection (LOD). sGP antigen capture ELISA with 2HG13 as the capture mAb and 2HG12-HRP as the detection mAb, the standard curve is shown. The LOD was calculated using a cutoff value of 2x background and was determined to be 95 ± 6.9 pg/mL (*n* = 3).

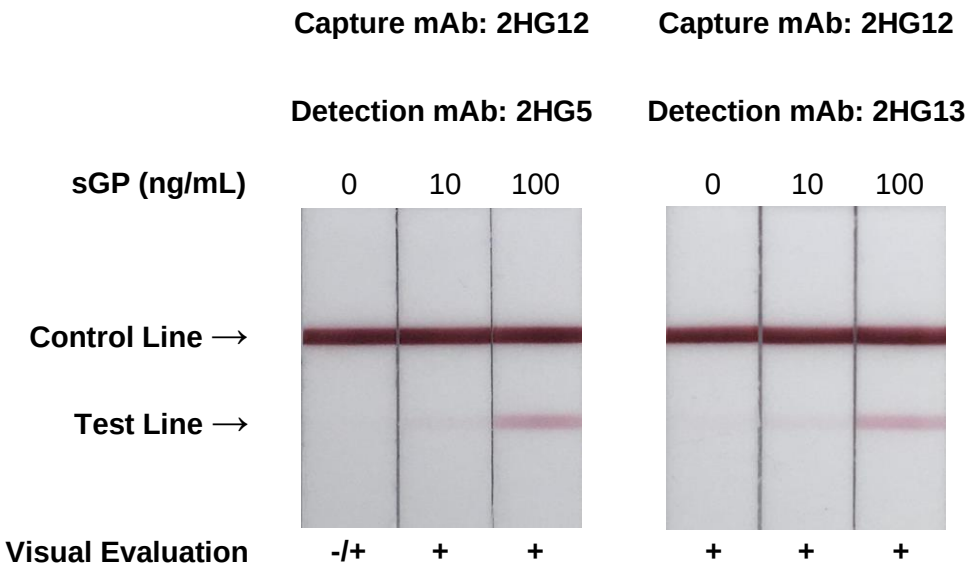

Figure 3. Lateral flow immunoassay prototypes 2HG12 as the capture mAb with 2HG5 detection (left) and 2HG13 detection (right) tested with recombinant sGP spiked into chase buffer at the indicated concentrations.

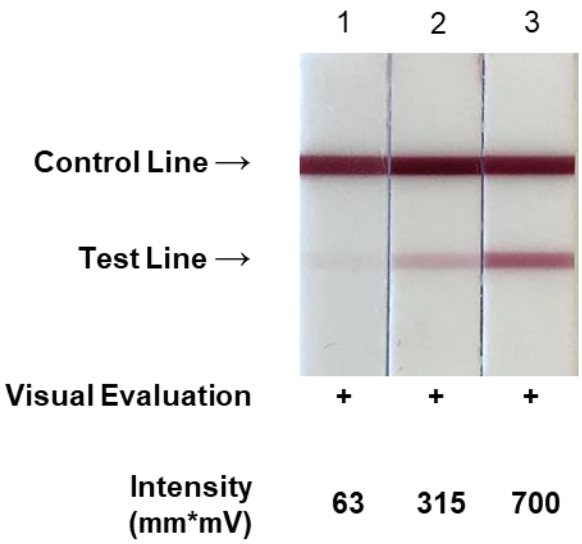

#	Sample Tested
1	Uninfected Vero E6 Cell Lysate*
2	Zaire Ebolavirus NR-49809 1 x 10^6 PFU/mL
3	Zaire Ebolavirus NR-49809 1 x 10^7 PFU/mL

*Unquantified

Figure 4. Testing of 2HG12 (capture) and 2HG5 (detection) LFI prototype with gamma-irradiated ZEBOV infected Vero E6 cell lysate.

CHAPTER 5

Conclusion

Melioidosis and Ebola virus disease (EVD) greatly contribute to the overall global burden of disease in resource limited areas. One of the most challenging aspects of diagnosing melioidosis and EVD is the need to correctly identify each pathogen early on in the course of the infection. The clinical manifestations of both diseases present as nonspecific in the early stages of infection making a diagnosis based on symptomology alone quite difficult. Clinicians must rely on more technically challenging and time-consuming diagnostics, such as culture and PCR, to validate the causative agent of the infection. This is challenging for both diseases as they are endemic in regions where specialized laboratories and highly trained personnel are not easily available. Melioidosis is treatable with antibiotics, though it necessitates the identification of *B. pseudomallei*, as the bacteria is intrinsically resistant to many frontline antibiotics. The gold standard of culture can take up to seven days to yield a result which can delay administration of life saving antibiotics. For EVD, there are antibody therapies, however they are not cost effective for the general population in Africa where infections are most common and are not very effective. Early identification of EVD is crucial to ensure patients are isolated thereby reducing the spread of the virus by the infected person. Currently, PCR is the gold standard, but there can be large time delays in acquiring results, especially during widespread outbreaks. Both diseases would greatly benefit from a rapid diagnostic that is sensitive enough to diagnose an infection early.

In the first study, a protocol was developed using magnetic particles for the enrichment of CPS in melioidosis patient samples. The concentration of CPS in patient samples can vary across several orders of magnitude. The AMD Plus LFI has a great limit of detection at

around 80-160 pg/mL, however CPS can be present at sub picogram levels within patient samples. Although CPS is a large molecule in comparison to the pore size for glomerular filtration, it is hypothesized that the rod-like structure of the molecule barrels into the pore on an axis allowing for filtration through the kidneys, thereby being excreted in the urine of infected patients. As such, urine appears to be an important matrix for the detection of CPS in melioidosis patients. Benefits of urine as the testing matrix include non-invasive collection and the ability to acquire large volumes making it more ideal than serum. The LFI is limited to a sample volume of about 150 µL, a fraction of what can be collected from a patient. It would be ideal to be able to analyze a larger volume of urine on the LFI to potentially detect CPS molecules that would otherwise go unused in the sample volume that is not able to be assessed on the LFI. To address this, a pretreatment protocol was developed that utilizes magnetic particles for the magnetic immunoprecipitation of CPS from a large sample volume and concentrated down to a volume that can be tested on the LFI. This protocol was developed using CPS spiked into buffer and normal human urine. The method was found to be successful in enhancing the intensity of the test line when analyzing increasingly larger volumes containing the same concentration of CPS. Importantly, employment of this protocol as a pretreatment step does not add much time and can still rapidly produce an AMD Plus LFI result. Confirmed melioidosis patient urine samples were available for testing and results validated that this protocol can successfully enrich samples, providing positive LFI results for samples that tested negative without enrichment. Overall, this protocol addressed the need of a more sensitive CPS detection method in patients who have concentrations of CPS in their urine that fall below the detection range of the AMD Plus LFI.

The second study evaluated an alternative pretreatment method utilizing concentrators that work passively to enrich samples for CPS. While the magnetic particle protocol from the first study discussed in Chapter 2 is an improvement for the detection of low concentrations of CPS, it does require multiple steps; however, it does not require any specialized equipment and does not add much time to produce a result. The Vivapore BJP-5/30 concentrators used in this study passively concentrate urine in an easy to use device that does not require any additional equipment. The time to concentrate throughout this study varied from minutes to 24 hours, which is considerably longer than magnetic immunoprecipitation, but is faster than culturing patient samples. This less hands-on approach for sample enrichment was successful in producing more positive AMD Plus LFI results when compared to nonconcentrated samples, and this pattern held true in the testing of cohorts across two endemic regions.

Both sample pretreatment protocols have the enhance the diagnosis of melioidosis, however, both are in early stages of development and evaluation of their utility. Further development of the magnetic immunoprecipitation protocol is essential to transition it from a clinical laboratory method to one that can be done at the POC. Development of a dropper-based system coupled with an inexpensive 3D printed sample tube apparatus to enclose an inexpensive magnet would make this more accessible to the rural areas where this bacterium is endemic. The evaluation of how robust the dissociation and neutralization steps can be would allow for this to be employed by a person who is otherwise untrained in diagnostic testing. In both studies, urine samples were filtered prior to using the pretreatment methods. This is not ideal, and testing needs to be conducted to determine the ability of these methods to function as expected with unfiltered samples. The research

conducted in both Chapters 2 and 3 indicate that enrichment for CPS prior to running the sample on the AMD Plus LFI, in one form or another, is a great alternative approach for the detection of CPS that could potentially lead to increased clinical sensitivity.

The final study focused on the development of a prototype lateral flow immunoassay for the detection of EBOV sGP to potentially diagnose EVD. A total of seventeen monoclonal antibodies were isolated and characterized by Western immunoblotting, ELISA, SPR, and LFI. Western immunoblotting validated that all mAbs were reactive to ZEBOV recombinant sGP and gamma-irradiated ZEBOV antigen preparations from infected Vero E6 cells in either reduced, non-reduced, or both conditions. An antigen-capture ELISA was developed using two mAbs from this library and optimized for the detection of sGP. This ELISA was determined to have a limit of detection of 95 pg/mL. The top eight mAbs were also characterized via SPR for their affinity and kinetics for sGP. With the exception of 1HG6, all mAbs characterized on this platform had similar affinities, though the binding kinetics varied. The mAb pairs that worked well in the ELISA also worked well in the LFI format, though it was not the same pair that was determined to be superior in both. The same pairs working well across multiple platforms is not always observed, but here it is most likely reflecting the spatially separate epitopes of sGP that these mAbs bind to. It appears that many of these mAbs in this library might potentially be recognizing epitopes in close proximity to each other, or even identical epitopes, as many pairs did not work in tandem. Regardless, a top pair for the LFI was identified and validated to detect sGP down to 10 ng/mL as well as be reactive to native protein in cell lysate from ZEBOV infected Vero E6 cells. The results from this initial characterization and testing of these mAbs

demonstrates great promise for the development of an sGP LFI for the rapid diagnosis of EVD, which is greatly needed.

Literature Cited

1. Whitmore, A. and C.S. Krishnaswami, *A Hitherto Undescribed Infective Disease in Rangoon.* The Indian medical gazette, 1912. **47**(7).

2. Galyov, E.E., P.J. Brett, and D. DeShazer, *Molecular insights into Burkholderia pseudomallei and Burkholderia mallei pathogenesis.* Annual review of microbiology, 2010. **64**.

3. Whitmore, A., *An Account of a Glanders-like Disease occurring in Rangoon.* The Journal of hygiene, 1913. **13**(1).

4. Stanton, A.T. and W. Fletcher, *Melioidosis, a new disease of the tropics.* Trans. Fourth Congr. Far East Assoc. Trop. Medicine, 1921(2): p. 196-198.

5. Yabuuchi, E., et al., *Proposal of Burkholderia gen. nov. and transfer of seven species of the genus Pseudomonas homology group II to the new genus, with the type species Burkholderia cepacia (Palleroni and Holmes 1981) comb. nov.* Microbiology and immunology, 1992. **36**(12).

6. Cheng, A.C. and B.J. Currie, *Melioidosis: epidemiology, pathophysiology, and management.* Clinical microbiology reviews, 2005. **18**(2).

7. Wagar, E., *Bioterrorism and the Role of the Clinical Microbiology Laboratory.* Clinical microbiology reviews, 2016. **29**(1).

8. Chaowagul, W., et al., *Melioidosis: a major cause of community-acquired septicemia in northeastern Thailand.* The Journal of infectious diseases, 1989. **159**(5).

9. Heng, B.H., et al., *Epidemiological surveillance of melioidosis in Singapore.* Annals of the Academy of Medicine, Singapore, 1998. **27**(4).

10. Ashdown, L.R. and R.W. Guard, *The prevalence of human melioidosis in Northern Queensland.* The American journal of tropical medicine and hygiene, 1984. **33**(3).

11. Dance, D.A., *Ecology of Burkholderia pseudomallei and the interactions between environmental Burkholderia spp. and human-animal hosts.* Acta tropica, 2000. **74**(2-3).

12. French, C.T., et al., *Virulence from the rhizosphere: ecology and evolution of Burkholderia pseudomallei-complex species.* Current opinion in microbiology, 2020. **54**.

13. Pumpuang, A., et al., *Survival of Burkholderia pseudomallei in distilled water for 16 years.* Transactions of the Royal Society of Tropical Medicine and Hygiene, 2011. **105**(10).

14. Ribolzi, O., et al., *Land use and soil type determine the presence of the pathogen Burkholderia pseudomallei in tropical rivers.* Environmental science and pollution research international, 2016. **23**(8).

15. Limmathurotsakul, D., et al., *Predicted global distribution of Burkholderia pseudomallei and burden of melioidosis.* Nat Microbiol, 2016. **1**: p. 15008.

16. Zehnder, A.M., et al., *Burkholderia pseudomallei isolates in 2 pet iguanas, California, USA.* Emerging infectious diseases, 2014. **20**(2).

17. Stewart, T., et al., *Epidemiology and investigation of melioidosis, Southern Arizona.* Emerging infectious diseases, 2011. **17**(7).

18. CDC. *2021 Multistate outbreak of melioidosis | Melioidosis | CDC*. 2021 2021-11-04T02:42:58Z; Available from: https://www.cdc.gov/melioidosis/outbreak/2021/index.html.

19. Cossaboom, C.M., et al., *Melioidosis in a Resident of Texas with No Recent Travel History, United States.* Emerging infectious diseases, 2020. **26**(6).

20. Dance, D.A., *Melioidosis as an emerging global problem.* Acta tropica, 2000. **74**(2-3).

21. Barnes, J.L. and N. Ketheesan, *Route of infection in melioidosis.* Emerging infectious diseases, 2005. **11**(4).

22. Limmathurotsakul, D., et al., *Increasing incidence of human melioidosis in Northeast Thailand.* The American journal of tropical medicine and hygiene, 2010. **82**(6).

23. Currie, B.J., et al., *Melioidosis epidemiology and risk factors from a prospective whole-population study in northern Australia.* Tropical medicine & international health : TM & IH, 2004. **9**(11).

24. Fong, S.M., et al., *Thalassemia major is a major risk factor for pediatric melioidosis in Kota Kinabalu, Sabah, Malaysia.* Clinical infectious diseases : an official publication of the Infectious Diseases Society of America, 2015. **60**(12).

25. Wiersinga, W.J., et al., *Melioidosis: insights into the pathogenicity of Burkholderia pseudomallei.* Nature reviews. Microbiology, 2006. **4**(4).

26. McLeod, C., et al., *Clinical presentation and medical management of melioidosis in children: a 24-year prospective study in the Northern Territory of Australia and review of the literature.* Clinical infectious diseases : an official publication of the Infectious Diseases Society of America, 2015. **60**(1).

27. Currie, B.J., *Melioidosis: evolving concepts in epidemiology, pathogenesis, and treatment.* Seminars in respiratory and critical care medicine, 2015. **36**(1).

28. Choy, J.L., et al., *Animal melioidosis in Australia.* Acta tropica, 2000. **74**(2-3).

29. Kingston, C.W., *Chronic or latent melioidosis.* The Medical journal of Australia, 1971. **2**(12).

30. Johnson, A.B. and N. Ali, *Reactivation of latent melioidosis.* Postgraduate medical journal, 1990. **66**(779).

31. Currie, B.J., et al., *Melioidosis: acute and chronic disease, relapse and re-activation.* Transactions of the Royal Society of Tropical Medicine and Hygiene, 2000. **94**(3).

32. Carroll, K.C., et al., *Jawetz, Melnick & Aldberg's Medical Microbiology*. 26 ed. 2013, New York: McGraw-Hill Medical.

33. Singh, M. and M. Mahmood, *Melioidosis: the great mimicker - University of Nevada, Reno.* Journal of Community Hospital Internal Medicine Perspectives, 2017. **7**(4): p. 245-247.

34. Cheng, A.C., et al., *Clinical definitions of melioidosis.* The American journal of tropical medicine and hygiene, 2013. **88**(3).

35. Kelser, E.A., *Melioidosis: a greater threat than previously suspected?* Microbes and infection, 2016. **18**(11).

36. Gibney, K.B., A.C. Cheng, and B.J. Currie, *Cutaneous melioidosis in the tropical top end of Australia: a prospective study and review of the literature.* Clinical infectious diseases : an official publication of the Infectious Diseases Society of America, 2008. **47**(5).

37. Wiersinga, W.J., et al., *Melioidosis.* Nat Rev Dis Primers, 2018. **4**: p. 17107.

38. Currie, B.J., L. Ward, and A.C. Cheng, *The epidemiology and clinical spectrum of melioidosis: 540 cases from the 20 year Darwin prospective study.* PLoS neglected tropical diseases, 2010. **4**(11).

39. Limmathurotsakul, D., et al., *Defining the true sensitivity of culture for the diagnosis of melioidosis using Bayesian latent class models.* PLoS One, 2010. **5**(8): p. e12485.

40. Wuthiekanun, V., et al., *Short Report: Quantitation of B. Pseudomallei in Clinical Samples.* Am. J. Trop. Med. Hyg., 2007. **77**(5): p. 812-813.

41. Wongsuvan, G., et al., *Lack of correlation of Burkholderia pseudomallei quantities in blood, urine, sputum, and pus.* Southeast Asian J Trop Med Public Health, 2009. **40**(4): p. 781–784.

42. Lau, S.K., et al., *Laboratory diagnosis of melioidosis: past, present and future.* Experimental biology and medicine (Maywood, N.J.), 2015. **240**(6).

43. Houghton, R.L., et al., *Development of a prototype lateral flow immunoassay (LFI) for the rapid diagnosis of melioidosis.* PLoS neglected tropical diseases, 2014. **8**(3).

44. Tandhavanant, S., et al., *Monoclonal antibody-based immunofluorescence microscopy for the rapid identification of Burkholderia pseudomallei in clinical specimens.* The American journal of tropical medicine and hygiene, 2013. **89**(1).

45. Tiyawisutsri, R., et al., *Antibodies from patients with melioidosis recognize Burkholderia mallei but not Burkholderia thailandensis antigens in the indirect hemagglutination assay.* Journal of clinical microbiology, 2005. **43**(9).

46. Gee, J.E., et al., *Use of 16S rRNA gene sequencing for rapid identification and differentiation of Burkholderia pseudomallei and B. mallei.* Journal of clinical microbiology, 2003. **41**(10).

47. Gilad, J., D. Schwartz, and Y. Amsalem, *Clinical features and laboratory diagnosis of infection with the potential bioterrorism agents burkholderia mallei and burkholderia pseudomallei.* International journal of biomedical science : IJBS, 2007. **3**(3).

48. Koh, S.F., et al., *Development of a multiplex PCR assay for rapid identification of Burkholderia pseudomallei, Burkholderia thailandensis, Burkholderia mallei and Burkholderia cepacia complex.* Journal of microbiological methods, 2012. **90**(3).

49. Hoffmaster, A.R., et al., *Melioidosis diagnostic workshop, 2013.* Emerg Infect Dis, 2015. **21**(2).

50. Suttisunhakul, V., et al., *Evaluation of Polysaccharide-Based Latex Agglutination Assays for the Rapid Detection of Antibodies to Burkholderia pseudomallei.* The American journal of tropical medicine and hygiene, 2015. **93**(3).

51. Pumpuang, A., et al., *Comparison of O-polysaccharide and hemolysin co-regulated protein as target antigens for serodiagnosis of melioidosis.* PLoS neglected tropical diseases, 2017. **11**(3).

52. Suttisunhakul, V., et al., *Development of Rapid Enzyme-Linked Immunosorbent Assays for Detection of Antibodies to Burkholderia pseudomallei.* Journal of clinical microbiology, 2016. **54**(5).

53. Phokrai, P., et al., *A Rapid Immunochromatography Test Based on Hcp1 Is a Potential Point-of-Care Test for Serological Diagnosis of Melioidosis.* Journal of clinical microbiology, 2018. **56**(8).

54. Khupulsup, K. and B. Petchclai, *Application of indirect hemagglutination test and indirect fluorescent antibody test for IgM antibody for diagnosis of melioidosis in Thailand.* The American journal of tropical medicine and hygiene, 1986. **35**(2).

55. Shaw, T., et al., *Performance evaluation of Active Melioidosis Detect-Lateral Flow Assay (AMD-LFA) for diagnosis of melioidosis in endemic settings with limited resources.* PloS one, 2018. **13**(3).

56. Robertson, G., et al., *Rapid diagnostics for melioidosis: a comparative study of a novel lateral flow antigen detection assay.* Journal of medical microbiology, 2015. **64**(8).

57. Podnecky, N.L., et al., *Efflux Pump-mediated Drug Resistance in Burkholderia.* Frontiers in Microbiology, 2015. **0**.

58. Leelarasamee, A. and S. Bovornkitti, *Melioidosis: review and update.* Reviews of infectious diseases, 1989. **11**(3).

59. Inglis, T.J., *The Treatment of Melioidosis.* Pharmaceuticals (Basel, Switzerland), 2010. **3**(5).

60. Dance, D., *Treatment and prophylaxis of melioidosis*, in *Int J Antimicrob Agents*. 2014. p. 310-8.

61. CDC. *History of Ebola Virus Disease (EVD) Outbreaks*. 2022 2022-01-10T03:12:32Z 1 Feb 2022]; Available from: https://www.cdc.gov/vhf/ebola/history/chronology.html.

62. WHO, *Ebola haemorrhagic fever in Sudan, 1976. Report of a WHO/International Study Team.* Bulletin of the World Health Organization, 1978. **56**(2).

63. WHO, *Ebola haemorrhagic fever in Zaire, 1976. Report of an International Commission.* Bulletin of the World Health Organization, 1978. **56**(2).

64. Cox, N.J., et al., *Evidence for two subtypes of Ebola virus based on oligonucleotide mapping of RNA.* The Journal of infectious diseases, 1983. **147**(2).

65. Okware, S.I., et al., *An outbreak of Ebola in Uganda.* Tropical medicine & international health : TM & IH, 2002. **7**(12).

66. Coltart, C.E., et al., *The Ebola outbreak, 2013-2016: old lessons for new epidemics.* Philosophical transactions of the Royal Society of London. Series B, Biological sciences, 2017. **372**(1721).

67. Groseth, A., H. Feldmann, and J.E. Strong, *The ecology of Ebola virus.* Trends in microbiology, 2007. **15**(9): p. 408-416.

68. Barrette, R.W., et al., *Discovery of Swine as a Host for the Reston ebolavirus.* Science, 2009. **325**(5937): p. 204-206.

69. Miranda, M.E., et al., *Epidemiology of Ebola (Subtype Reston) Virus in the Philippines, 1996.* The Journal of Infectious Diseases, 1999. **179**(Supplement_1): p. S115-S119.

70. Miranda, M.E.G., et al., *Seroepidemiological study of filovirus related to Ebola in the Philippines.* The Lancet, 1991. **337**(8738): p. 425-426.

71. B., J.P., et al., *Preliminary report: isolation of Ebola virus from monkeys imported to USA.* The Lancet, 1990. **335**(8688): p. 502-505.

72. Jacob, S.T., et al., *Ebola virus disease.* Nature reviews. Disease primers, 2020. **6**(1).

73. Smit, M.A., et al., *Characteristics and Outcomes of Pediatric Patients With Ebola Virus Disease Admitted to Treatment Units in Liberia and Sierra Leone: A*

Retrospective Cohort Study. Clinical infectious diseases : an official publication of the Infectious Diseases Society of America, 2017. **64**(3).

74. Feldmann, H. and T.W. Geisbert, *Ebola haemorrhagic fever.* Lancet (London, England), 2011. **377**(9768).

75. Okoror, L., et al., *Transplacental transmission: A rare case of Ebola virus transmission.* Infectious disease reports, 2018. **10**(3).

76. Leroy, E.M., et al., *Fruit bats as reservoirs of Ebola virus.* Nature, 2005. **438**(7068).

77. Franz, D.R., et al., *Clinical recognition and management of patients exposed to biological warfare agents.* Clinics in laboratory medicine, 2001. **21**(3).

78. Vogel, G., *Infectious Diseases. Testing new Ebola tests.* Science (New York, N.Y.), 2014. **345**(6204).

79. Towner, J.S., et al., *Rapid diagnosis of Ebola hemorrhagic fever by reverse transcription-PCR in an outbreak setting and assessment of patient viral load as a predictor of outcome.* Journal of virology, 2004. **78**(8).

80. Zaki, S.R. and C.S. Goldsmith, *Pathologic features of filovirus infections in humans.* Current topics in microbiology and immunology, 1999. **235**.

81. Rowe, A.K., et al., *Clinical, virologic, and immunologic follow-up of convalescent Ebola hemorrhagic fever patients and their household contacts, Kikwit, Democratic Republic of the Congo. Commission de Lutte contre les Epidémies à Kikwit.* The Journal of infectious diseases, 1999. **179 Suppl 1**.

82. CDC. *Treatment | Ebola (Ebola Virus Disease) | CDC*. 2021 2021-02-26T04:30:48Z; Available from: https://www.cdc.gov/vhf/ebola/treatment/index.html.

83. Saxena, D., et al., *Atoltivimab/maftivimab/odesivimab (Inmazeb) combination to treat infection caused by Zaire ebolavirus.* Drugs of today (Barcelona, Spain : 1998), 2021. **57**(8).

84. Lee, A., *Ansuvimab: First Approval.* Drugs, 2021. **81**(5).

85. Clark, D.V., P.B. Jahrling, and J.V. Lawler, *Clinical management of filovirus-infected patients.* Viruses, 2012. **4**(9).

86. FDA, *First FDA-approved vaccine for the prevention of Ebola virus disease, marking a critical milestone in public health preparedness and response | FDA*. 2019, U.S. Food & Drug Administration.

87. Marzi, A., et al., *VSV-EBOV rapidly protects macaques against infection with the 2014/15 Ebola virus outbreak strain.* Science, 2015. **349**(6249): p. 739-742.

88. FDA, *Statistical Review - ERVEBO*, U.S.F.D. Administration, Editor. 2019, United States Food & Drug Administration: https://www.fda.gov/vaccines-blood-biologics/ervebo.

89. Parkin, J. and B. Cohen, *An overview of the immune system.* Lancet (London, England), 2001. **357**(9270).

90. Murphy, K., *Janeway's Immunobiology*. 8 ed. 2012, New York: Garland Science, Taylor & Francis Group, LLC.

91. Brezski, R.J. and J.G. Monroe, *B-cell receptor.* Advances in experimental medicine and biology, 2008. **640**.

92. Schroeder, H.W. and L. Cavacini, *Structure and function of immunoglobulins.* The Journal of allergy and clinical immunology, 2010. **125**(2 Suppl 2).

93. Cohen, S., *Antibody structure.* Journal of clinical pathology. Supplement (Association of Clinical Pathologists), 1975. **6**.

94. Franklin, E.C., *Structure and function of immunoglobulins.* Acta endocrinologica. Supplementum, 1975. **194**.

95. Coutelier, J.P., et al., *Virally induced modulation of murine IgG antibody subclasses.* | *Journal of Experimental Medicine* | *Rockefeller University Press.* Journal of Experimental Medicine, 1988. **168**(6): p. 2373-2378.

96. Darwish, I.A., *Immunoassay Methods and their Applications in Pharmaceutical Analysis: Basic Methodology and Recent Advances.* International journal of biomedical science : IJBS, 2006. **2**(3).

97. Wild, D., *The Immunoassay Handbook: Theory and Applications of Ligand Binding, ELISA and Related Techniques,*. 2013: Jordon Hill: Elsevier Science & Technology.

98. Koczula, K.M. and A. Gallotta, *Lateral flow assays.* Essays in biochemistry, 2016. **60**(1).

99. Gnoth, C. and S. Johnson, *Strips of Hope: Accuracy of Home Pregnancy Tests and New Developments.* Geburtshilfe und Frauenheilkunde, 2014. **74**(7).

100. Black, M.A., et al., *Analytical performance of lateral flow immunoassay for SARS-CoV-2 exposure screening on venous and capillary blood samples.* Journal of immunological methods, 2021. **489**.

101. Posthuma-Trumpie, G.A., J. Korf, and A. van Amerongen, *Lateral flow (immuno)assay: its strengths, weaknesses, opportunities and threats. A literature survey.* Analytical and bioanalytical chemistry, 2009. **393**(2).

102. Quesada-González, D. and A. Merkoçi, *Nanoparticle-based lateral flow biosensors.* Biosensors & bioelectronics, 2015. **73**.

103. Wang, J.J., et al., *Rapid lateral flow tests for the detection of SARS-CoV-2 neutralizing antibodies.* Expert review of molecular diagnostics, 2021. **21**(4).

104. Apilux, A., et al., *Development of competitive lateral flow immunoassay coupled with silver enhancement for simple and sensitive salivary cortisol detection.* EXCLI journal, 2018. **17**.

105. Peruski, A.H. and L.F. Peruski, *Immunological methods for detection and identification of infectious disease and biological warfare agents.* Clinical and diagnostic laboratory immunology, 2003. **10**(4).

106. Payne, W.J., et al., *Clinical laboratory applications of monoclonal antibodies.* Clinical microbiology reviews, 1988. **1**(3).

107. Kaushik, A., et al., *Towards detection and diagnosis of Ebola virus disease at point-of-care.* Biosensors & bioelectronics, 2016. **75**.

108. Engvall, E. and P. Perlmann, *Enzyme-linked immunosorbent assay (ELISA). Quantitative assay of immunoglobulin G.* Immunochemistry, 1971. **8**(9).

109. Currie, B.J. and M. Kaestli, *Epidemiology: A global picture of melioidosis.* Nature, 2016. **529**(7586): p. 290-1.

110. Wiersinga, W.J., B.J. Currie, and S.J. Peacock, *Melioidosis.* N Engl J Med, 2012. **367**(11): p. 1035-44.

111. White, N.J., *Melioidosis.* Lancet, 2003. **361**(9370): p. 1715-22.

112. Fonseka, C.L., et al., *Acute pulmonary melioidosis presenting with multiple bilateral cavitary lesions in a healthy young adult: an authentic case report from Sri Lanka.* BMC Res Notes, 2016. **9**: p. 360.

113. Conrad, A., et al., *Multifocal melioidosis with femoral osteomyelitis in a healthy 25-year-old traveller.* BMJ Case Rep, 2016. **2016**.

114. Bodilsen, J., H. Langgaard, and H.L. Nielsen, *Cutaneous melioidosis in a healthy Danish man after travelling to South-East Asia.* BMJ Case Rep, 2015. **2015**.

115. Sirisinha, S., et al., *Recent developments in laboratory diagnosis of melioidosis.* Acta Trop, 2000. **74**(2-3): p. 235-45.

116. Wuthiekanun, V., et al., *Quantitation of B. Pseudomallei in clinical samples.* Am J Trop Med Hyg, 2007. **77**(5): p. 812-3.

117. Rhodes, K.A. and H.P. Schweizer, *Antibiotic resistance in Burkholderia species.* Drug Resist Updat, 2016. **28**: p. 82-90.

118. Lipsitz, R., et al., *Workshop on treatment of and postexposure prophylaxis for Burkholderia pseudomallei and B. mallei Infection, 2010.* Emerging infectious diseases, 2012. **18**(12).

119. Koczula, K.M. and A. Gallotta, *Lateral flow assays.* Essays Biochem, 2016. **60**(1): p. 111-20.

120. Nayak, S., et al., *Point-of-Care Diagnostics: Recent Developments in a Connected Age.* 2016.

121. Chaowagul, W., et al., *Empirical cephalosporin treatment of melioidosis.* Clin Infect Dis, 1999. **28**(6): p. 1328.

122. Marchetti, R., et al., *Burkholderia pseudomallei Capsular Polysaccharide Recognition by a Monoclonal Antibody Reveals Key Details toward a Biodefense Vaccine and Diagnostics against Melioidosis.* ACS Chem Biol, 2015. **10**(10): p. 2295-302.

123. Heiss, C., et al., *Structural analysis of capsular polysaccharides expressed by Burkholderia mallei and Burkholderia pseudomallei.* Carbohydr Res, 2012. **349**: p. 90-4.

124. DeMers, H., *Antibody-based diagnostics and therapeutics for Zaire ebolavirus and Burkholderia pseudomallei*. 2018, University of Nevada, Reno.

125. Burtnick, M.N., et al., *Development of capsular polysaccharide-based glycoconjugates for immunization against melioidosis and glanders.* Front Cell Infect Microbiol, 2012. **2**.

126. Nualnoi, T., et al., *In vivo Distribution and Clearance of Purified Capsular Polysaccharide from Burkholderia pseudomallei in a Murine Model*, in *PLoS Negl Trop Dis*. 2016.

127. Hall, C.M., et al., *Burkholderia pseudomallei, the causative agent of melioidosis, is rare but ecologically established and widely dispersed in the environment in Puerto Rico*, in *PLoS Negl Trop Dis*. 2019.

128. Peacock, S.J., et al., *Management of accidental laboratory exposure to Burkholderia pseudomallei and B. mallei.* Emerging infectious diseases, 2008. **14**(7).

129. Suputtamongkol, Y., et al., *Risk factors for melioidosis and bacteremic melioidosis.* Clinical infectious diseases : an official publication of the Infectious Diseases Society of America, 1999. **29**(2).

130. Meumann, E.M., et al., *Clinical features and epidemiology of melioidosis pneumonia: results from a 21-year study and review of the literature.* Clinical infectious diseases : an official publication of the Infectious Diseases Society of America, 2012. **54**(3).

131. Wiersinga, W.J., B.J. Currie, and S.J. Peacock, *Melioidosis.* The New England journal of medicine, 2012. **367**(11).

132. Currie, B.J., et al., *Endemic melioidosis in tropical northern Australia: a 10-year prospective study and review of the literature.* Clinical infectious diseases : an official publication of the Infectious Diseases Society of America, 2000. **31**(4).

133. Khakhum, N., I. Chapartegui-González, and A.G. Torres, *Combating the great mimicker: latest progress in the development of Burkholderia pseudomallei vaccines.* Expert review of vaccines, 2020. **19**(7).

134. Chakravorty, A. and C.H. Heath, *Melioidosis: An updated review.* Australian journal of general practice, 2019. **48**(5).

135. White, N.J., et al., *Halving of mortality of severe melioidosis by ceftazidime.* Lancet (London, England), 1989. **2**(8665).

136. Kumar, A., et al., *Duration of hypotension before initiation of effective antimicrobial therapy is the critical determinant of survival in human septic shock.* Critical care medicine, 2006. **34**(6).

137. Khosravi, Y., et al., *Antimicrobial susceptibility and genetic characterisation of Burkholderia pseudomallei isolated from Malaysian patients.* TheScientificWorldJournal, 2014. **2014**.

138. Kaestli, M., et al., *Comparison of TaqMan PCR assays for detection of the melioidosis agent Burkholderia pseudomallei in clinical specimens.* Journal of clinical microbiology, 2012. **50**(6).

139. Limmathurotsakul, D., et al., *Enzyme-linked immunosorbent assay for the diagnosis of melioidosis: better than we thought.* Clinical infectious diseases : an official publication of the Infectious Diseases Society of America, 2011. **52**(8).

140. Lew, A.E. and P.M. Desmarchelie r, *Detection of Pseudomonas pseudomallei by PCR and hybridization.* Journal of clinical microbiology, 1994. **32**(5).

141. Rizzi, M.C., et al., *Evaluation of the Active Melioidosis Detect™ test as a point-of-care tool for the early diagnosis of melioidosis: a comparison with culture in Laos.* Transactions of the Royal Society of Tropical Medicine and Hygiene, 2019. **113**(12).

142. Nuti, D.E., et al., *Identification of circulating bacterial antigens by in vivo microbial antigen discovery.* mBio, 2011. **2**(4).

143. Wiersinga, W.J., et al., *Melioidosis: insights into the pathogenicity of Burkholderia pseudomallei.* Nature Reviews Microbiology, 2021. **4**(4): p. 272-282.

144. Warawa, J.M., et al., *Role for the Burkholderia pseudomallei capsular polysaccharide encoded by the wcb operon in acute disseminated melioidosis.* Infection and immunity, 2009. **77**(12).

145. Perry, M., B., et al., *Structural characterization of the lipopolysaccharide O antigens of Burkholderia pseudomallei.* Infection and immunity, 1995. **63**(9).

146. Ruggiero, A., et al., *Paradoxical glomerular filtration of carbon nanotubes.* Proceedings of the National Academy of Sciences of the United States of America, 2010. **107**(27).

147. McLellan, L.K. and D.A. Hunstad, *Urinary Tract Infection: Pathogenesis and Outlook.* Trends in molecular medicine, 2016. **22**(11).

148. Foxman, B., *Urinary tract infection syndromes: occurrence, recurrence, bacteriology, risk factors, and disease burden.* Infectious disease clinics of North America, 2014. **28**(1).

149. Flores-Mireles, A.L., et al., *Urinary tract infections: epidemiology, mechanisms of infection and treatment options.* Nature reviews. Microbiology, 2015. **13**(5).

150. Reckseidler-Zenteno, S.L., R. DeVinney, and D.E. Woods, *The capsular polysaccharide of Burkholderia pseudomallei contributes to survival in serum by reducing complement factor C3b deposition.* Infection and immunity, 2005. **73**(2).

151. Woods, K.L., et al., *Evaluation of a Rapid Diagnostic Test for Detection of Burkholderia pseudomallei in the Lao People's Democratic Republic.* Journal of clinical microbiology, 2018. **56**(7).

152. Choi, J.Y., et al., *Burkholderia pseudomallei Detection among Hospitalized Patients, Sarawak.* The American journal of tropical medicine and hygiene, 2020. **102**(2).

153. Goeijenbier, M., et al., *Ebola virus disease: a review on epidemiology, symptoms, treatment and pathogenesis.* The Netherlands journal of medicine, 2014. **72**(9).

154. Baseler, L., et al., *The Pathogenesis of Ebola Virus Disease.* Annual review of pathology, 2017. **12**.

155. Goldstein, T., et al., *The discovery of Bombali virus adds further support for bats as hosts of ebolaviruses.* Nature Microbiology, 2018. **3**(10): p. 1084-1089.

156. Shultz, J.M., et al., *Distinguishing epidemiological features of the 2013-2016 West Africa Ebola virus disease outbreak.* Disaster health, 2016. **3**(3).

157. CDC. *Transmission | Ebola Hemorrhagic Fever | CDC*. 2021 2021-01-14T07:38:43Z; Available from: https://www.cdc.gov/vhf/ebola/transmission/index.html.

158. Broadhurst, M.J., T.J. Brooks, and N.R. Pollock, *Diagnosis of Ebola Virus Disease: Past, Present, and Future.* Clinical microbiology reviews, 2016. **29**(4).

159. Team, W.E.R. and B.P. Aylward B, Bawo L, Bertherat E, Bilivogui P, et al., *Ebola virus disease in West Africa--the first 9 months of the epidemic and forward projections.* The New England journal of medicine, 2014. **371**(16).

160. Dhillon, R.S., et al., *Ebola control: rapid diagnostic testing.* The Lancet. Infectious diseases, 2015. **15**(2).

161. *Revocation of Authorization of Emergency Use of an In Vitro Diagnostic Device for Detection of Ebola Virus*, F.a.D. Adminsitration, Editor. 2018: Federal Register. p. 37813-37816.

162. Madara, J.J., et al., *The multifunctional Ebola virus VP40 matrix protein is a promising therapeutic target.* Future virology, 2015. **10**(5).

163. Becquart, P., et al., *Identification of continuous human B-cell epitopes in the VP35, VP40, nucleoprotein and glycoprotein of Ebola virus.* PloS one, 2014. **9**(6).

164. Murphy, C., *Recent Advances in the Diagnosis and Management of Ebola Virus Disease.* Clinical Microbiology Newsletter, 2019. **41**(21): p. 185-189.

165. Wonderly, B., et al., *Comparative performance of four rapid Ebola antigen-detection lateral flow immunoassays during the 2014-2016 Ebola epidemic in West Africa.* PloS one, 2019. **14**(3).

166. DeMers, H.L., et al., *Development of an antigen detection assay for early point-of-care diagnosis of Zaire ebolavirus.* PLoS neglected tropical diseases, 2020. **14**(11).

167. Jain, S., et al., *Structural and Functional Aspects of Ebola Virus Proteins.* Pathogens (Basel, Switzerland), 2021. **10**(10).

168. Mehedi, M., et al., *A new Ebola virus nonstructural glycoprotein expressed through RNA editing.* Journal of virology, 2011. **85**(11).

169. Volchkov, V.E., et al., *GP mRNA of Ebola virus is edited by the Ebola virus polymerase and by T7 and vaccinia virus polymerases.* Virology, 1995. **214**(2).

170. Falzarano, D., et al., *Structure-function analysis of the soluble glycoprotein, sGP, of Ebola virus.* Chembiochem : a European journal of chemical biology, 2006. **7**(10).

171. Zhu, W., et al., *The Roles of Ebola Virus Soluble Glycoprotein in Replication, Pathogenesis, and Countermeasure Development.* Viruses, 2019. **11**(11).

172. Sanchez, A., et al., *Detection and molecular characterization of Ebola viruses causing disease in human and nonhuman primates.* The Journal of infectious diseases, 1999. **179 Suppl 1**.

173. Nualnoi, T., et al., *Immunoglobulin G subclass switching impacts sensitivity of an immunoassay targeting Francisella tularensis lipopolysaccharide.* PloS one, 2018. **13**(4).